



Disentangling the environmental processes responsible for the world's largest farmed fish-killing harmful algal bloom: Chile, 2016



Jorge I. Mardones ^{a,b,*}, Javier Paredes ^a, Marcos Godoy ^{c,d,e}, Rudy Suarez ^{c,d,f}, Luis Norambuena ^a, Valentina Vargas ^a, Gonzalo Fuenzalida ^a, Elias Pinilla ^g, Osvaldo Artal ^g, Ximena Rojas ^h, Juan José Dorantes-Aranda ⁱ, Kim J. Lee Chang ^j, Donald M. Anderson ^k, Gustaaf M. Hallegraeff ⁱ

^a Centro de Estudios de Algas Nocivas (CREAN), Instituto de Fomento Pesquero (IFOP), Puerto Montt, Chile

^b Centro FONDAP de Investigación en Dinámica de Ecosistemas Marinos de Altas Latitudes (IDEAL), Valdivia, Chile

^c Centro de Investigaciones Biológicas Aplicadas (CIBA), Puerto Montt, Chile

^d Laboratorio de Biotecnología Aplicada, Facultad de Medicina Veterinaria, Sede de la Patagonia, Puerto Montt 5480000, Chile

^e Doctorado en acuicultura, Programa cooperativo Universidad de Chile, Universidad Católica del Norte, Pontificia Universidad Católica de Valparaíso, Chile

^f Magíster en acuicultura, Universidad Católica del Norte, Coquimbo, Chile

^g CTPA-Putemán, Instituto de Fomento Pesquero (IFOP), Castro, Chile

^h Instituto Tecnológico del Salmón (INTESAL), Juan Soler Manfredini 41, Of. 1802, Puerto Montt, Chile

ⁱ Institute for Marine and Antarctic Studies (IMAS), University of Tasmania, Australia

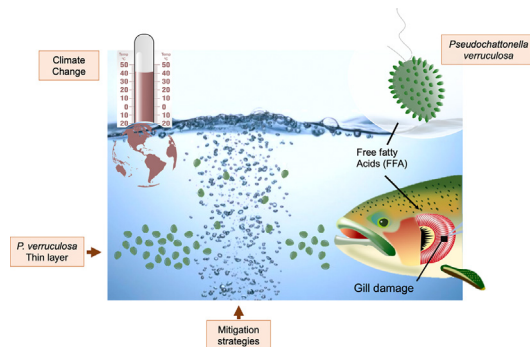
^j CSIRO Ocean and Atmosphere, GPO Box 1538, Hobart, TAS 7001, Australia

^k Biology Department, Woods Hole Oceanographic Institution (WHOI), Woods Hole, MA, USA

HIGHLIGHTS

- The largest farmed fish mortality ever recorded in the world was caused by *P. verruculosa* in Chile.
- Low flushing rates in Reloncaví Sound may lead to long lasting *P. verruculosa* blooms.
- Monitoring programs might have highly underestimated *P. verruculosa* cell densities in 2016.
- Cultured *P. verruculosa* is toxic only at extremely high cell densities and after cell rupture.
- Current mitigation methods used by Chilean salmon farms are not efficient for *P. verruculosa* blooms.

GRAPHICAL ABSTRACT



ARTICLE INFO

Article history:

Received 13 November 2020

Received in revised form 4 December 2020

Accepted 4 December 2020

Available online 25 December 2020

Editor: Daniel A. Wunderlin

Keywords:

Pseudochattonella verruculosa

Life cycle

ABSTRACT

The dinophyte microalga *Pseudochattonella verruculosa* was responsible for the largest farmed fish mortality ever recorded in the world, with losses for the Chilean salmon industry amounting to US\$ 800 M in austral summer 2016. Super-scale climatic anomalies resulted in strong vertical water column stratification that stimulated development of a dynamic *P. verruculosa* thin layer (up to 38 µg chl a L⁻¹) for several weeks in Reloncaví Sound. Hydrodynamic modeling (MIKE 3D) indicated that the Sound had extremely low flushing rates (between 121 and 200 days) in summer 2016. Reported algal cell densities of 7000–20,000 cells mL⁻¹ generated respiratory distress in fish that was unlikely due to low dissolved oxygen (permanently >4 mg L⁻¹). Histological examination of salmon showed that gills were the most affected organ with significant tissue damage and circulatory disorders. It is possible that some of this damage was due to a diatom bloom that preceded the *Pseudochattonella* event, thereby rendering the fish more susceptible to *Pseudochattonella*. No correlation between magnitude of

* Corresponding author at: Centro de Estudios de Algas Nocivas (CREAN), Instituto de Fomento Pesquero (IFOP), Puerto Montt, Chile.

E-mail address: jorge.mardones@ifop.cl (J.I. Mardones).

Thin layer
Ichthyotoxicity
Fish mortality
Mitigation strategies

fish mortality and algal cell abundance nor fish age was evident. Algal cultures revealed rapid growth rates and high cell densities (up to 600,000 cells mL⁻¹), as well as highly complex life cycle stages that can be easily overlooked in monitoring programs. In cell-based bioassays, Chilean *P. verruculosa* was only toxic to the RTgill-W1 cell line following exposures to high cell densities of lysed cells (>100,000 cells mL⁻¹). Fatty acid profiles of a cultured strain showed elevated concentrations of potentially ichthyotoxic, long-chain polyunsaturated fatty acids (PUFAs) (69.7% ± 1.8%)- stearidonic (SDA, 18:4ω3-28.9%), and docosahexaenoic acid (DHA, 22:6ω3-22.3%), suggesting that lipid peroxidation may help to explain the mortalities, though superoxide production by *Pseudochattonella* was low (< 0.21 ± 0.19 pmol O₂⁻ cell⁻¹ h⁻¹). It therefore remains unknown what the mechanisms of salmon mortality were during the *Pseudochattonella* bloom. Multiple mitigation strategies were used by salmon farmers during the event, with only delayed seeding of juvenile fish into the cages and towing of cages to sanctuary sites being effective. Airlift pumping, used effectively against other fish-killing HABs in the US and Canada was not effective, perhaps because it brought subsurface layers of *Pseudochattonella* to the surface, or and it also may have lysed the fragile cells, rendering them more lethal. The present study highlights knowledge gaps and inefficiency of contingency plans by the fish farming industry to overcome future fish-killing algal blooms under future climate change scenarios. The use of new technologies based on molecular methods for species detection, good farm practices by fish farms, and possible mitigation strategies are discussed.

© 2020 Elsevier B.V. All rights reserved.

1. Introduction

The sea-cage rearing of salmonids in Chile began in the 1980s and soon after the industry grew to become the second largest global producer of farmed salmon, with an annual production of over 700,000 metric tons after 2011 (Avendaño-Herrera, 2018). To date, most salmon farming is located in Reloncaví Sound and inner Chiloé Island channels of the Los Lagos Region. There is also fish farming further south in the Aysén Region and ongoing expansion to the Magallanes Region. The first setback of the Chilean industry caused by a harmful algal bloom (HAB) occurred in 1988 because of an outbreak of the raphidophyte *Heterosigma* that killed >5000 tons of salmon with economic losses estimated at US\$11 M (Mardones et al., 2012). Since then, fish-killing algal (FKA) blooms have increased in intensity, frequency and specially in diversity with the region (Mardones, 2020). Among the fish killing microalgal species along the Chilean coast (e.g., *Alexandrium catenella*, *Heterosigma akashiwo* and *Karenia selliformis*), the dictyochophyte *Pseudochattonella verruculosa* was responsible for the worst damage from a HAB in Chile's history, with massive socio-economic impacts in 2016. This event is considered the largest farmed fish mortality ever recorded in the world with losses estimated at 100,000 metric tons of Atlantic salmon (*Salmo salar*), Coho salmon (*Oncorhynchus kisutch*) and rainbow trout (*Oncorhynchus mykiss*), corresponding to a expected export loss of US\$800 million (approximately 15% of Chile's yearly production) (Trainer et al., 2019).

Two species of this dictyochophyte genus have been described so far, *P. farcimen* Eikrem, Edvardsen and Thronsen, and *P. verruculosa* (Y. Hara and Chihara) Hosoi-Tanabe, Honda, Fukaya, Otake, Inagaki and Sako (Hosoi-Tanabe et al., 2007; Edvardsen et al., 2007; Eikrem et al., 2009). Both *Pseudochattonella* species are recognized as ichthyotoxic after producing fish-kills in Japan (Yamamoto and Tanaka, 1990; Baba et al., 1995; Imai et al., 1998), Northern Europe (Lu and Goebel, 2000; Naustvoll et al., 2002; Edvardsen et al., 2007; Riisberg and Edvardsen, 2008), and New Zealand (MacKenzie et al., 2011; Chang et al., 2014). The New Zealand *Pseudochattonella*, however, appears to be a hybrid species as it contains a dominant genetic background of *P. verruculosa* related to the large subunit ribosomal DNA (LSU) and plastid rbcL sequences and mitochondrial- COI genetic material from *P. farcimen* (Chang et al., 2014).

In Chile, *P. verruculosa* (initially referred to as *Chattonella aff. verruculosa*) is currently the only *Pseudochattonella* species formally identified using the LSU nuclear marker (Mardones et al., 2019). Since its first report in 2004, this species has been detected regularly in low cell densities, except for the massive outbreak in 2016 and the latest salmon mortality (138 tons) recorded in Chiloé Island (Pilpilehue) in March 2019 (Mardones et al., 2012, 2019). The maximum *P. verruculosa* cell densities

during the 2016 event ranged from 7000 to 20,000 cells mL⁻¹. The bloom was associated with extraordinary inshore and ocean water conditions in late 2015 and early 2016 because of a positive phase of the Southern Annular Mode (SAM) and a strong El Niño event that changed the atmospheric circulation in the SE Pacific Ocean (Clément et al., 2016; León-Muñoz et al., 2018). The reduction in freshwater contribution during this large-scale anomaly allowed advection of more saline offshore waters, which was suggested as a key trigger for the massive *P. verruculosa* bloom (Mardones et al., 2019).

The toxic mode of action in *Pseudochattonella* is still unknown but most inspections of affected fish have shown impairment to the gills (Andersen et al., 2015). For instance, Skjelbred et al. (2011) observed decreased performance of the gills in salmon smolts (*Salmo salar*) and cod (*Gadus morhua*) exposed to extreme cell densities of 1–3 × 10⁷ cells L⁻¹ of *P. verruculosa*. However, these Scandinavian authors were unable to show any acute mortality although gill tissue showed a variety of lesions. A few studies have also reported liver problems after exposure to *P. verruculosa* (MacKenzie et al., 2011; M. Svendsen, per. Comm.). The threshold in cell density needed to induced anomalies in fish seems to be species and even strain specific. For *Pseudochattonella farcimen*, harmful cell abundance has been estimated as 500 cells mL⁻¹ (Andersen et al., 2015), whilst *P. verruculosa* has been estimated to be more toxic in New Zealand and Chile, with dangerous thresholds in cell density claimed to be as low as 10 and 1 cell mL⁻¹, respectively (MacKenzie et al., 2011; Montes et al., 2018).

Numerous studies performed on embryos, gill cells, model organisms and whole fish have pointed to differing arguments with regard to toxicity. Skjelbred et al. (2011) showed that microalgal extracts of *P. verruculosa* and *P. farcimen* produced damage to the cell membrane of primary hepatocytes and metabolism inhibition in embryo cells but no acute toxicity on the nauplii of brine shrimp (*Artemia leach*). In feeding experiments with rotifers, Chang et al. (2014) observed the release of cellular material and undigested food across their oral cavities when exposed to whole *P. cf. verruculosa* cells. Likewise, Andersen et al. (2015) suggested that live *Pseudochattonella* cells are needed to produce a noxious effect on fish. In cytotoxicity experiments using the RTgill-W1 assay, only very high *P. verruculosa* densities of 100,000 cells mL⁻¹ produced 80–65% decrease in gill cell viability, with no significant differences between lysed cells and supernatant (Mardones et al., 2019).

The active ichthyotoxic metabolites synthesized by *Pseudochattonella* have not yet been described. Free fatty acids (FFA), possibly involving a synergistic effect with reactive oxygen species (ROS) have been suggested as the primary mechanism for the raphidophyte *Chattonella* which, however, produces up to 100-fold more ROS than other algae (Marshall et al., 2005). *Pseudochattonella* belongs to the class Dictyochophyceae and is not

related to the class Raphidophyceae (Hosoi-Tanabe et al., 2007; Edvardsen et al., 2007), so its ichthyotoxic mode of action could be different.

Both species of *Pseudochattonella* show variable cell morphology (elongated to spherical) and size (4–34 µm) varying in response to growth phases and environmental conditions, making them extremely difficult to identify in routine monitoring (Eckford-Soper and Daugbjerg, 2016). Cell fixation using standard fixatives such as Lugol's iodine, needed for preservation in sample transport, can make things worse and raise the question whether cell counts and species identifications have been performed correctly in the past. Molecular-based methods

(i.e., dot blot hybridization, PCR, qPCR and microarray) might be useful tools to improve an early warning of *Pseudochattonella* species, but molecular sequence data is still limited for *Pseudochattonella* in Chile.

The present study provides a multi-disciplinary data analysis of the massive 2016 *P. verruculosa* fish-killing event based on: (1) *in situ* measurements during the HAB (phytoplankton, oceanographic and atmospheric data), (2) pathology exhibited by affected fish; (3) mitigation strategies attempted at the salmon farms and (4) *in vitro* laboratory studies on cultured *Pseudochattonella* strains (phylogenetic position, life cycle characteristics, cell growth under different temperatures that mimic the 2016 water column and ichthyotoxicity). Knowledge gaps

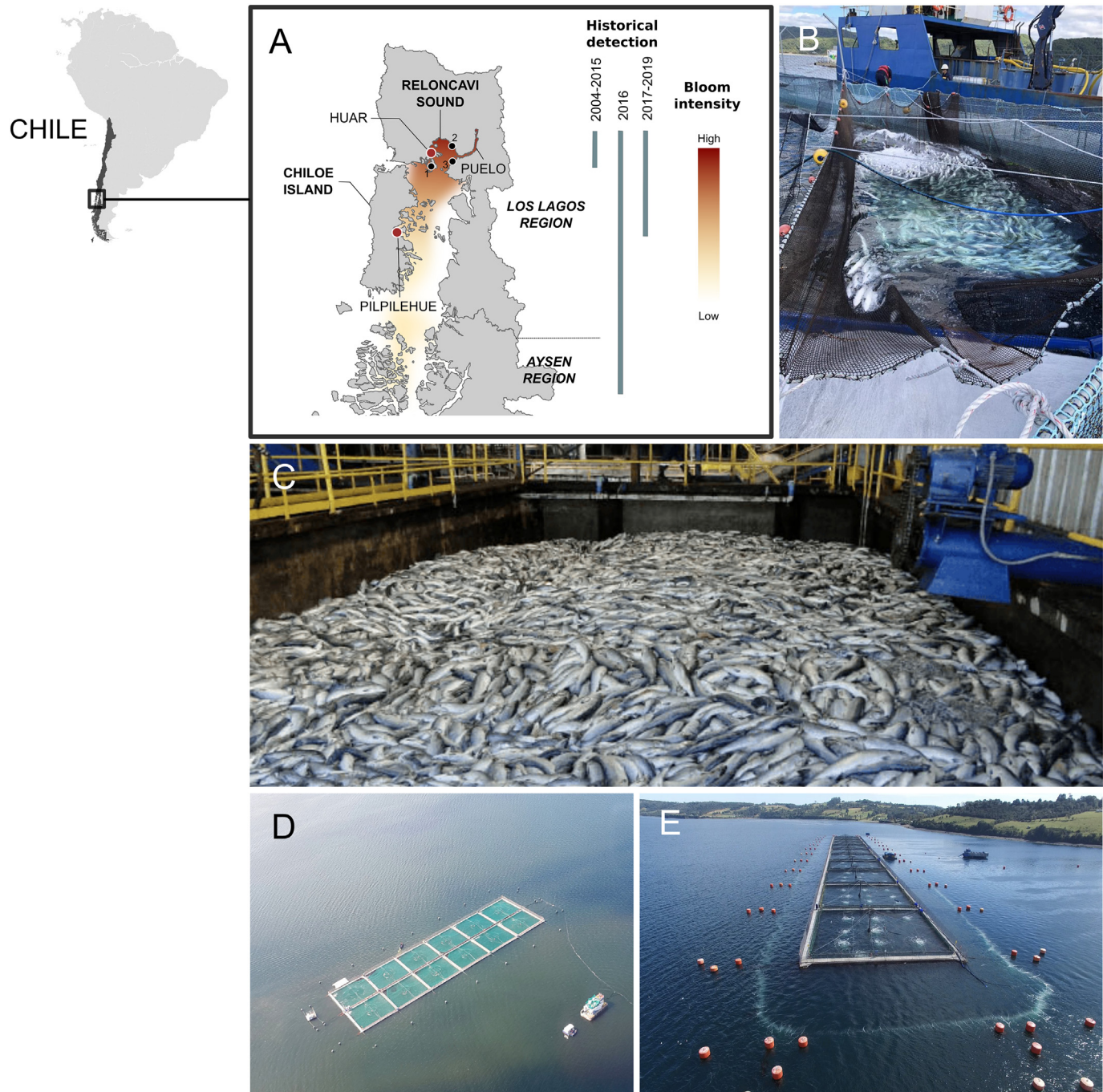


Fig. 1. A) Study area in the Chilean southern fjords showing location of isolation of the *P. verruculosa* strains used in this study (red circles) and the biogeographic distribution of historical bloom events recorded between 2004 and 2019. Red-yellow colour bar represents *P. verruculosa* bloom intensity during the 2016 fish-kill event; B-C) Examples of fish-kills during *Pseudochattonella* bloom events in southern Chile; B) Pilpilehue (Chiloé Island), March 2019, photo: SERNAPESCA and C) Reloncaví Sound, Feb-Mar 2016, photo: SERNAPESCA; D) Water discoloration at an affected salmon farm impacted by *P. verruculosa*, photo: M. Godoy; E) Airlift upwelling and bubble curtains used as a mitigation strategy against the 2016 *P. verruculosa* bloom event, photo: INTESAL.

and future research priorities to address future fish-killing algal blooms in Chilean fjords are also discussed.

2. Materials and method

2.1. Study area

Reloncaví Sound is situated in the northern region of the Patagonian fjords (41.42°S , 72.50°W) (Fig. 1A). The Sound is ~42 km long (N-S axis), has a surface of ~1150 km² and a maximum depth of >300 m. The water circulation in the Sound is mostly influenced by freshwater contribution from the Puelo River with an average streamflow of $650 \text{ m}^3 \text{ s}^{-1}$ and a pluvio-nival regime (Alves-de-Souza et al., 2019). The elevated freshwater input in this system produced by rainfalls and/or snow melts causes stratification of the water column as a result of strong vertical salinity gradient. Vertical stratification restricts nutrient interchange between the surface (brackish, dissolved silicic acid-rich) and deep (oceanic nitrate/orthophosphate-rich) layers of the water column (González et al., 2013). The interplay of these masses of water not only modulates a characteristic seasonal fluctuation in primary production but also intensive salmon farming activities.

2.2. Field studies during the 2016 *P. verruculosa* bloom

2.2.1. Phytoplankton sampling and identification

Within the frame of the INTESAL phytoplankton monitoring program, water samples were regularly collected at 82 monitoring sites every week from January to March 2016. Sea surface (0–1 m) water samples were collected with plastic container and preserved with buffered Lugol's iodine solution (0.5–1% final concentration). Responding to the need to render microalgae cell counts in near real time during the bloom event, counts of live cells from gently shaken unpreserved samples were also adopted. The shaking seemed to induce the microalgae cells immotile, appropriately long for rapid counts. Subsamples (1 mL) were analyzed using a Sedgewick Rafter chamber and toxic *Pseudochattonella* cells counted with an inverted microscope. *Pseudochattonella verruculosa* was the only ichthyotoxic species present in sufficiently high abundance to justify this mass fish-killing event.

2.2.2. Oceanographic and atmospheric data and numerical modeling

Water salinity (PSU), temperature (°C), chlorophyll-a ($\mu\text{g L}^{-1}$) and dissolved oxygen -DO (mg L^{-1} and % saturation) (profiles of ~30 m) were obtained from the IFOP's monitoring program using a Seabird 19 CTD-F/O instrument at 3 selected sampling stations (St.1 = Calbuco; St.2 = Metri and St.3 = Caicura) on a monthly basis on 12th–15th January, 16th–17th February and 17th–18th March (bloom period). The hydrodynamic MIKE 3D FM model was implemented to estimate the water circulation in the study area according to Pinilla et al. (2020). Briefly, the licensed MIKE 3D FM (flexible mesh) model (developed by DHI, 2016) considers limited volumes to define mathematical solutions of three-dimensional incompressible Reynolds averaged Navier-Stokes equations. The MIKE 3D FM model was configurated with bathymetric information obtained from the Servicio Hidrográfico de la Armada de Chile (www.shoa.cl) and river discharges from the Dirección General de Aguas (www.dga.cl). Atmospheric conditions at the northern Patagonian fjords were modeled with the non-hydrostatic model WRF v. 3.5.1 (Skamarock et al., 2008) nested in the National Centers for Environmental Prediction (NCEP) operational system. Based on hydrodynamic modeling, transport time scales in the study area were determined using the 'flushing time' method. According to Takeoka (1984) and Monsen et al. (2002), flushing time is described as the time required for a total mass of a material within an area of interest (i.e., fjord or bay) to reduce to a factor of e^{-1} (~37%). Flushing time values were vertically integrated and arranged in 5 categories within the 'water retention index (WRI)'. Meridional wind anomaly was analyzed with the ERA5 product (Hersbach et al., 2020). ERA5 is the fifth generation of ECMWF

atmospheric reanalysis for global climate with a resolution of 31 km. The meridional wind anomaly was estimated from the difference between the 2016 wind summer average and the wind summer average from 1979 to 2018. The sea surface temperature (SST) anomaly was assessed with the Visible and Infrared Imager/Radiometer Suite (VIIRS-SNPP). SNPP is the primary spacecraft in this series, and VIIRS is the successor to MODIS for Earth science data products (Xiong et al., 2014). VIIRS has a spatial resolution of 0.25° and 22 spectral bands varying from 412 nm to $12 \mu\text{m}$. The SST summer anomaly was calculated similar to the meridional wind anomaly, but using data from 2012 to 2020.

2.2.3. Salmon farms data and fish pathology

In order to assess fish mortality losses and efficacy of the mitigation strategies adopted by the salmon farming companies during the *P. verruculosa* event, phone or email surveys were carried out with technical staff and managers of 10 salmon-farming companies affected by the HAB event, between February 22 and March 24, 2016. The questionnaire included fish species, fish weight (g), fish density at the cages (kg m^{-3}), fish mortality (%), maximum *in situ* *Pseudochattonella* cell counts (cells mL^{-1}) and mitigation strategy used. The survey represented 76% (34 out of 45) of total salmon farms with fish mortality associated with *P. verruculosa*, according to the Chilean National Fisheries Service (SERNAPESCA).

Moribund fish ($n=107$) were collected from 37 affected salmon farms during and after the *P. verruculosa* bloom in order to check macroscopic morphological alterations and for tissue sampling according to Noga (2000). The salmon were dissected and tissue sections fixed in 10% buffered formalin for histopathological analysis. The tissue sections contained gill, liver, heart, intestine, kidney, red muscle and spleen. Tissue samples (3–4 μm) were stained with hematoxylin and eosin for histological examination following Evensen and Lorenzen (1997).

2.3. Post-bloom laboratory studies

2.3.1. *Pseudochattonella* cultures

Five mono-clonal cultures of the ichthyotoxic dictyochophyte *Pseudochattonella verruculosa* were isolated from two outbreaks that occurred in 2016 (1 strain) and 2019 (4 strains) in the northern Patagonian fjords (Table 1). Non-axenic cultures were kept in culture at the Center for Harmful Algal studies in Puerto Montt, Chile (CREAN-IFOP) and were grown in L1 medium at 15 °C in sterile filtered (0.22 μm) seawater at 30 salinity and $100 \mu\text{mol photon m}^{-2} \text{ s}^{-1}$ light (cool white fluorescence lamps) under a 16:8 h light:dark cycle. Live cells from field samples and different stages of the life cycle from monoclonal cultures were examined and photographed with an inverted light microscope (Zeiss Axio Vert.A1 and MoticAE31E). The sizes of cells were measured using the software Motic® Image Plus 2.0.

2.3.2. *Pseudochattonella* phylogeny

The large subunit (LSU) rDNA D1-D2 region and large subunit of ribulose bisphosphate carboxylase (*rbcL*) of monoclonal cultures of five Chilean *P. verruculosa* were sequenced. Cells from monoclonal cultures of the CREAN_PV01, CREAN_PV03, CREAN_PV04, CREAN_PV05, CREAN_PV06 strains were collected at the exponential growth phase, pelleted by centrifugation at 1500g at 4 °C for 10 min. The cell pellets were later incubated in 10 mL Proteinase K (10 mg mL^{-1}) and 1 mL CTB buffer at 65 °C for 3 h. The LSU (D1-D2) region was amplified using the primers D1R and D2C (Scholin et al., 1994; Edvardsen et al., 2003) and the *rbcL* gene using the primers PrL1 and NDrcS (Daugbjerg and Henriksen, 2001). The PCR procedure included: 1) a denaturation step of 95 °C for 1 min, 2) 35 cycles of 95 °C for 30 s, 3) 56 °C for 30 s, 4) 72 °C for 30 s and 7 min extension at 72 °C. For the *rbcL* gene, an annealing temperature of 50 °C was used. After visualization on a 1.5% agarose gel and purification using a gel band purification kit (GE Healthcare) and the Illustra GFX PCR DNA, the PCR products of both genes were sent to Macrogen Korea for sequencing. The ClustalW/

Table 1

Location and date of isolation of the *Pseudochattonella* cultures used in this study.

Strain	Region/locality	Isolated by	Isolation date	Salmon mortality associated
CREAN_PV01 ^a	Los Lagos/Huar Is.	A. Martin	March 2016	100,000 tons/15% of Chile's yearly production
CREAN_PV03	Los Lagos/Pilpilhue	J.I. Mardones	March 2019	150 tons/59,917 units
CREAN_PV04	Los Lagos/Pilpilhue	J.I. Mardones	March 2019	
CREAN_PV05	Los Lagos/Pilpilhue	J.I. Mardones	March 2019	
CREAN_PV06	Los Lagos/Pilpilhue	J.I. Mardones	March 2019	

^a Original code: ARC498.

Geneious Prime 2019.0.3 software was used for sequences alignment with sequences available in GenBank (Larkin et al., 2007). Maximum likelihood analyses (ML) and identification of appropriate models of sequence evolution (LSU and ITS: GTR + I) were performed using PhyML (Guindon et al., 2010) and jModeltest (Posada, 2008), respectively. The Likelihood Ratio Test (aLRT, Anisimova and Gascuel, 2006) and bootstrap analysis (1000 replicates) were used to estimate node reliability and MrBayes V3.1.2 for Bayesian analyses (Ronquist and Huelsenbeck, 2003).

2.3.3. Growth of *P. verruculosa* at different temperatures

All strains of *P. verruculosa* were used to evaluate growth performance at temperatures of 12, 15 and 18 °C. At the beginning of the experiment, an initial density of 500 cells/mL was inoculated into Erlenmeyer flasks containing 100 mL of filtered seawater (34 in salinity) enriched with L1 medium. Each treatment per strain was performed in triplicate. The experiment was performed for 28 days with microalgae samples collected every 4 days. For cell density estimations, microalgae samples were fixed with glutaraldehyde 4% immediately after sampling and counted under an inverted light microscope (Motic AE31E). The culture treatments were maintained at 45 µmol photon m⁻² s⁻¹ (cool white fluorescence lamps) under a 16:8 h light:dark cycle. Growth rates were determined through a linear regression model $\gamma_i = \alpha + \beta\chi_i$ (Guillard and Hargraves, 1993), where $\gamma_i = \ln$ -transformed cell density (cells mL⁻¹); χ_i = time (days); α = intercept; and β = growth rate (d⁻¹). Growth rate was estimated between t day 0 and 8 for all strains and temperatures. Cell density at the end of the exponential phase was used as the maximum cell density response (cells mL⁻¹).

2.3.4. HPLC chlorophyll analysis

A detailed description of pigments analysis using HPLC is provided by Mardones et al. (2020). Briefly, for chlorophyll *a* (chl *a*) quantification, 50 mL of the five *P. verruculosa* cultures in exponential phase of growth were filtered (5.0 µm SVPP) and extracted in 1 mL acetone (100%) after sonication and soaking (24 h) as described by Chang et al. (2003). Chl *a* quantification at 446 nm was performed using a Shimadzu high resolution liquid chromatograph (HPLC), with SPD-M20A diode array detector (DAD) following Sanz et al. (2015).

2.3.5. Production of superoxide anion by *P. verruculosa*

A detailed description of the method used for superoxide anion estimation is provided by Mardones et al. (2020). Briefly, lysed cultures and intact algal cells of *P. verruculosa* CREAN_PV01 were assessed for production of superoxide anion following Godrant et al. (2009). In a 96-well microplate, 270 mL of *Pseudochattonella* culture kept at 17 °C at 100 µmol photon m⁻² s⁻¹ under a 12:12 h L:D cycle was mixed with 3 mL of xanthine at 5 mM. For blank correction, 3 mL of superoxide dismutase at 5 kU L⁻¹ were used. A standard curve was prepared using 3 standard solutions of xanthine oxidase at 0.1, 0.4 and 0.7 U L⁻¹. A microplate reader (FLUOstar OPTIMA) was used to screen luminescence for 20 min after adding 5 mL of 6-(4-methoxyphenyl)-2-methyl-3,7-dihydroimidazo[1,2-*a*]pyrazin-3(7H)-one hydrochloride at 125 mM.

2.3.6. Lipid analysis

A detailed description of the method used for lipid analysis is provided by Mardones et al. (2020). Briefly, filters containing the

P. verruculosa CREAN_PV01 strain were extracted with a mixed solution of dichloromethane/methanol/water (1:2:0.8, v/v/v) as described by Mooney et al. (2007). The lipids were transmethylated in a mixed solution of methanol/chloroform/hydrochloric acid (10:1:1, v/v/v) for 2 h at 85 °C. In order to obtain fatty acid methyl esters (FAME) after water addition, the mixture was extracted 3 times with a mixed solution of hexane/chloroform (4:1, v/v) under a stream of nitrogen gas. Samples were analyzed by gas chromatography–mass spectrometry (GC–MS) using an Agilent Technologies 7890 N GC (Palo Alto, CA, USA). FAME were classified by evaluation against retention times of laboratory standard solutions.

2.3.7. RTgill-W1 cell line assay

A detailed description of the RTgill-W1 cell line assay to test cytotoxicity in microalgae is provided by Mardones et al. (2020). Briefly, the RTgill-W1 cell line was obtained from the American Type Culture Collection (ATCC). For routine conservation, cells were cultured in the dark at 17 °C in 25-cm² culture-treated flasks with L-15 medium, supplemented with 10% (v/v) fetal bovine serum, and an antibiotic-antimycotic containing penicillin (10,000 units mL⁻¹), amphotericin B (25 mg mL⁻¹) and streptomycin (10 mg mL⁻¹). 0.25% trypsin– 0.02% EDTA was used to detach cells from the bottom of the flask. The cytotoxicity assay from lysed and live cells of *P. verruculosa* was performed using 96 multi-well microplates according to Dorantes-Aranda et al. (2011). The lysed cells treatment examined the cytotoxic effect of potential intra-cellular toxins and the whole cell experiment assessed extra-cellular toxins actively released by the cells as well as the effect of direct contact of *P. verruculosa* on gill cells. Both lysed and whole cells treatments used *P. verruculosa* (CREAN_PV01) cultures at 15 °C in sterile filtered seawater (0.22 µm; 30 psu) at 100 µmol photon m⁻² s⁻¹ under a 12:12 h L:D cycle were used for cytotoxic experiments. After detachment, gill cells were adjusted to a density of 2×10^5 cells mL⁻¹. Then, gill cells were seeded in 96-well flat bottom microplates in quadruplicate per treatment, using a volume of 100 µL per well. After gill cell attachment in the dark at 17 °C for 48 h, L-15 medium was removed, the gill cells rinsed with phosphate buffer saline and exposed to 100 µL of the experimental microalgae treatments. Live *Pseudochattonella* cells treatments were prepared from two cultures (CREAN_PV01 and CREAN_PV03) in the exponential phase of growth at 6 cell densities (1 to 100,000 cells mL⁻¹) and the exposure to the gill cells was performed in the dark at 17 °C for 4 h. Lysed *P. verruculosa* cells treatments were prepared from cultures in the exponential phase of growth at 5 cell densities (10 to 100,000 cells mL⁻¹). The lysed cell solution was prepared by sonication of diluted samples for 10 min at 17 °C and then filtered by a filter of 0.22 µm. The exposure of *P. verruculosa* intracellular metabolites was performed for 1, 2, 4 and 6 h in the dark at 17 °C. In order to assess cell viability, gill cells were incubated for 2 h in the dark using L-15/ex medium, containing 5% of the indicator dye alamarBlue (Pagé et al., 1993; Dayeh et al., 2005). After incubation, the medium was removed and gill cells were rinsed with phosphate buffer saline. The fluorescence of AlamarBlue was detected using a microplate reader (FLUOstar Omega) with emission and excitation filters of 590 and 540 nm, respectively. The gill cells viability was stated as percentage of the treatments versus the controls (% of control).

2.4. Statistical analysis

To assess the effect of temperature and the intraspecific response of the five *P. verruculosa* strains, analysis of variance (ANOVA) on specific growth rate, maximum cell density and cytotoxicity to the gill cell line, was carried out. Normality was assessed by the Shapiro-Wilk test and homogeneity of variances by the Levene's test. To determine pairwise growth differences among strains, a *post hoc* analysis using a Tukey HSD test was performed. The null hypothesis was rejected in all statistical analyses under a significance *p*-value of 0.01. All analyses were carried out using the software R v. 3.0.1 (Ihaka and Gentleman, 1996).

3. Results

3.1. Field data

3.1.1. *P. verruculosa* bloom development

Phytoplankton sampling between 21 and 24 January 2016, a few days after the fish kills commenced, revealed the presence of a small golden-brown flagellate on the eastern coast of Chiloé Island, later identified as *P. verruculosa* (Fig. 2A). By the end of January, *P. verruculosa* cell densities did not exceed 100 cells mL⁻¹ and moved northwards reaching Reloncaví Sound (Fig. 2B). Over the two following weeks, however, cell numbers at

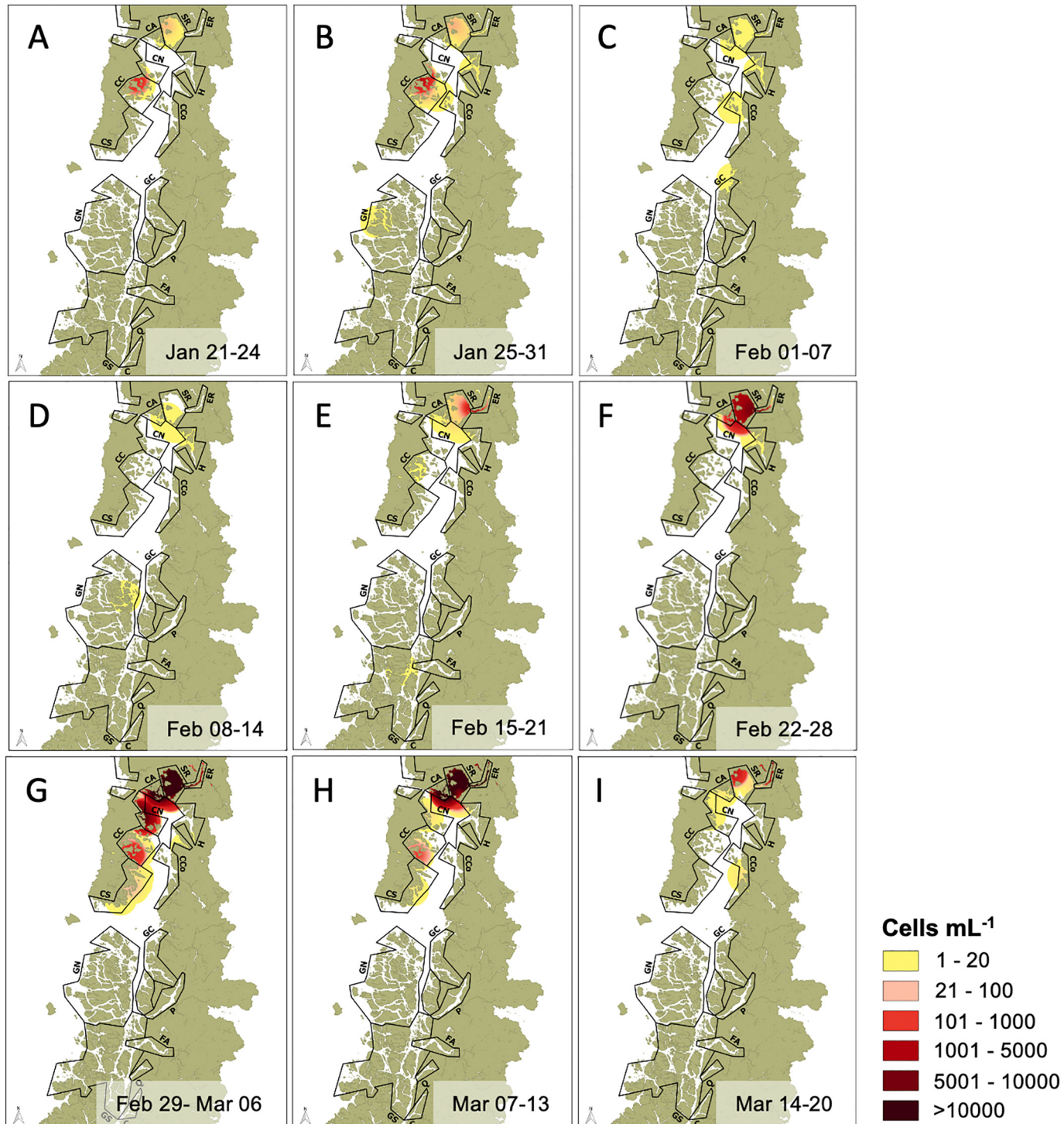


Fig. 2. Weekly *P. verruculosa* cell abundance (cells mL⁻¹) at 0 m recorded between the 21st of January until the 20th of March 2016 in Los Lagos and Aysén Regions.

the farm sites decreased ($<20 \text{ cells mL}^{-1}$) and showed an apparent dispersion of the bloom to the southern Aysén region (Fig. 2D). On 15 February, cells numbers rapidly increased in Reloncaví Sound ($>100 \text{ cells mL}^{-1}$) concurrent with a surge in fish deaths (Fig. 2E). Bloom cell densities of $>1000 \text{ cells mL}^{-1}$ related to mass salmon mortalities (max. 39,942 tons) started on 22nd February (Fig. 2F). Between 29 February and 13

mL^{-1}) concurrent with a surge in fish deaths (Fig. 2E). Bloom cell densities of $>1000 \text{ cells mL}^{-1}$ related to mass salmon mortalities (max. 39,942 tons) started on 22nd February (Fig. 2F). Between 29 February and 13

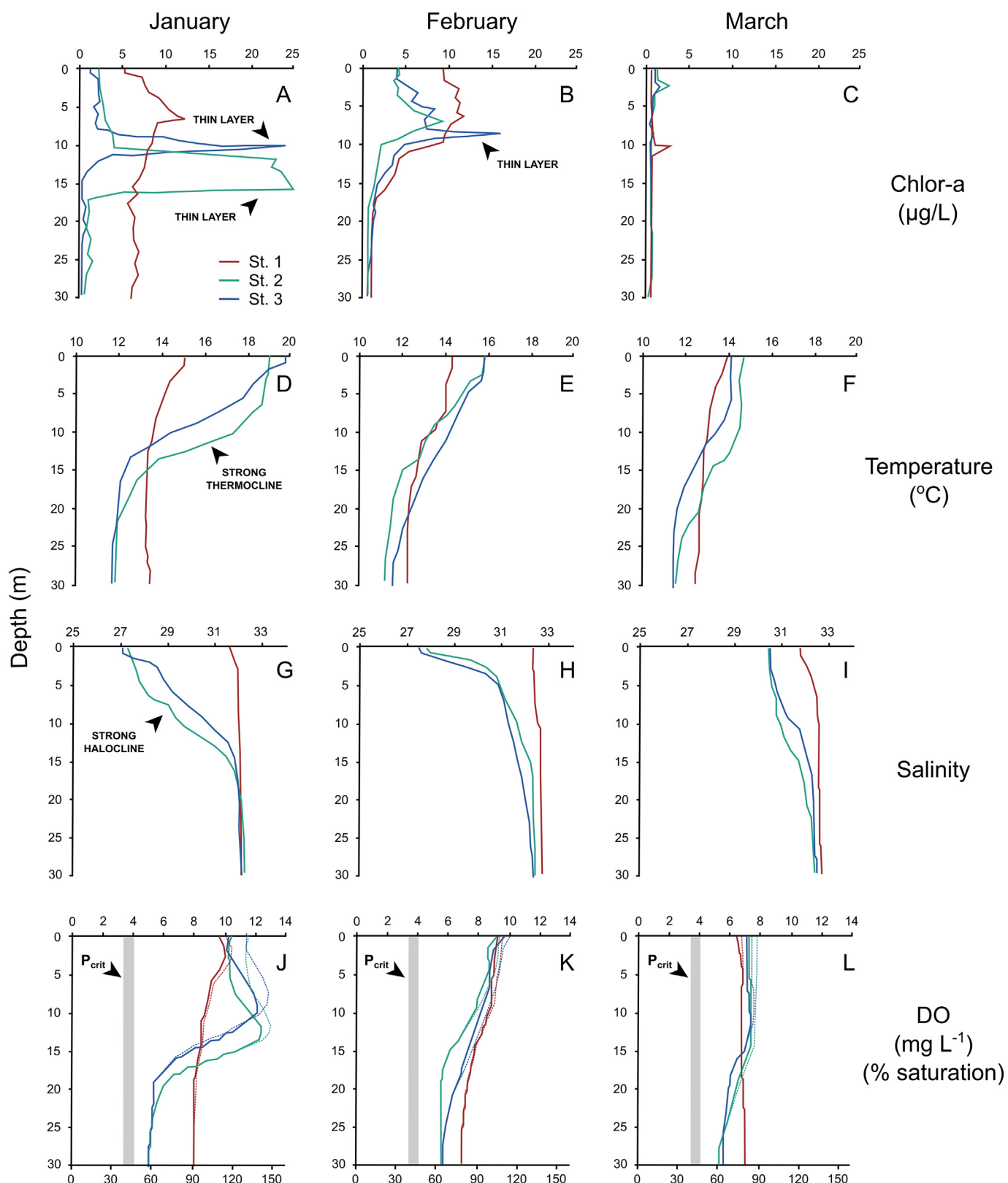


Fig. 3. Monthly CTD-F/O profiles from the Reloncaví Sound at stations 1 to 3 during the 2016 *Pseudochattonella* bloom event. A–C) Chlorophyll a (black arrows show thin layer formation); D–F) Temperature (black arrow shows strong thermocline at stations 2 and 3); G–I) Salinity (black arrow shows strong halocline at stations 2 and 3) and J–L) Dissolved oxygen concentration (continuous line; mg L^{-1} in the top X axis) and % saturation (dashed line; bottom X axis), black arrows show the critical oxygen threshold (P_{crit}) for *Salmo salar* according to Barnes et al. (2011). Colour code for sampling stations is shown in panel A) and applies to all panels.

March, the outbreak reached its peak with cell counts exceeding 10,000 cells mL⁻¹ (Fig. 2G–H). After 14 March, cell abundance steadily declined and the phytoplankton assemblage gradually became controlled by diatoms.

3.1.2. Oceanographic and atmospheric data and modeled water retention index (WRI)

The CTD-F/O data of the water column during the bloom period from 3 stations located in Reloncaví Sound are presented in Fig. 3. In January, CTD-F/O profiles showed that stations located at the inner portion of Reloncaví Sound (St. 2 and 3 nearby Reloncaví fjord) were highly stratified with a surface temperature/salinity of 19 °C/27.5, which supported a high subsurface peak of Chl *a* (concentration of ~25 µg L⁻¹) between 10 and 17 m depth (thin layers). In the southwest station 1, the water column was deeply mixed (~14–15 °C and ~32 in salinity) and peak Chl *a* concentration was ~13 µg L⁻¹ at 6 m depth (Fig. 3A, D and G). In February, the thermo-halocline in stations 2 and 3 shallowed with surface temperatures around 15.8 °C and salinities of 27 (Fig. 3E–H). The Chl *a* peak shallowed and decreased in intensity at both stations with concentrations from 9 to 16 µg L⁻¹ (Fig. 3B). The southernmost station 1 slightly decreased in surface temperature and salinity but increased in surface Chl *a* compared to January. By March 2016, the water column was mixed and Chl *a* was low (<3 µg L⁻¹) in all sampling stations. Dissolved oxygen (DO) was permanently above 60% saturation throughout the water column at the 3 sampling sites between January and March. Maximum DO concentrations of ~12 mg L⁻¹ (~130% saturation) were associated with maximum sub-surface Chl *a* concentrations (thin layers) (Fig. 3J–L).

Using the VIIRS-SNPP, the SST summer anomaly for 2016 at Reloncaví Sound was estimated as ~ +1 °C (Fig. 4A). The ERA5 product showed a positive meridional wind anomaly of ~0.5 m s⁻¹ with a north direction at the Reloncaví Sound during summer 2016 (Fig. 4B).

The water retention index (WRI) for the inner sea of northern Patagonia, based on hydrodynamic modeling (MIKE 3D), is shown in Fig. 4C. The modeled WRI values ranged between 1 and 4 with the highest value of 4 estimated for Reloncaví Sound and the Comau fjord. This result estimates that the water residence time in Reloncaví Sound, where the maximum *P. verruculosa* cell density was recorded in 2016, was between 121 and 200 days. Water retention for fjords such as Reloncaví and Reñihué were estimated at 61–120 days (WRI = 3), while the rest of the inner Chiloé sea areas did not exceed 60 days (WRI = 1 and 2).

3.1.3. Fish farms data and fish histopathology

Among the 34 surveyed fish farms (76% of total affected farms) during the *P. verruculosa* bloom event, a total of 70.6% of the cages were Atlantic salmon (*Salmo salar*), 26.5% Coho salmon (*Oncorhynchus kisutch*) and 2.9% rainbow trout (*Oncorhynchus mykiss*). Around 88% of cages maintained a fish density of ~15 kg m⁻³ and the estimated fish weight average per cage ranged between 200 and 3000 g. The number of fish per cage varied between ~170, 000 to 1,000,000 with mortality losses between 8 and 100%. *Pseudochattonella* cell counts performed by farmers at the cages ranged between 620 and 30,000 cells mL⁻¹. No correlation was observed between the magnitude of fish mortality (%) and *P. verruculosa* cell counts ($R^2=0.06$) or fish weight ($R^2=0.04$) (Fig. 5C and D, respectively).

Five mitigation strategies were attempted at the salmon farms including: towing of net pens ($n = 11$), seeding delay ($n = 6$), withholding feed ($n = 10$), tarpaulin skirts ($n = 6$) and aeration systems ($n = 30$). The latter was the most used mitigation strategy among farmers (47.6%). The most effective strategies were fish relocation (72.7%) and fish seeding delay (66.7%) whilst tarpaulin skirts and aeration were the least effective (0%). (Fig. 5E).

Salmon affected by the *P. verruculosa* outbreak presented signs of respiratory distress prior to death including gasping near the water

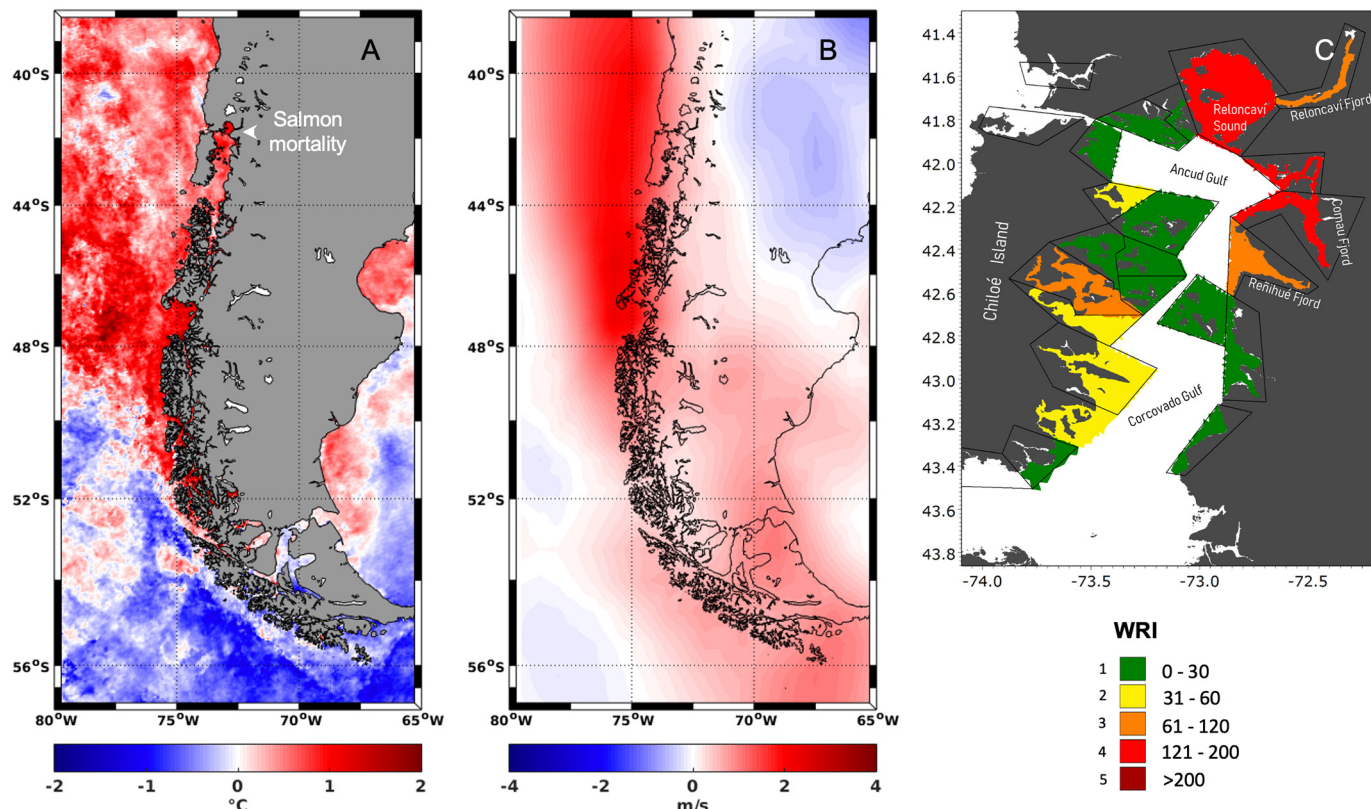


Fig. 4. Mesoscale oceanographic conditions for the Patagonian coast during the 2016 *Pseudochattonella* bloom event. A) Sea surface temperature anomaly (2012–2019), B) Meridional wind anomaly (1979–2018) showing a north forward flow (positive values) and C) Water retention index (WRI) based on the hydrodynamic MIKE 3D FM model for the northernly Patagonian basins and fjords.

surface, swimming upside down (loss of balance) with mouth and operculum open (Fig. 6A). The main macroscopic findings relate to the presence of multifocal to diffuse hemorrhages and discoloration of the branchial apex (Fig. 6B). Histological examination of fish tissues showed that the gills were the most affected organ with circulatory disorders such as telangiectasia, thrombosis, and branchial edema (Fig. 6C-D).

Additionally, interlamellar hyperplasia was observed, with partial and complete fusion of the branchial lamellae and formation of interlamellar vacuoles, occasionally associated with spongiosis and hyperplasia of the mucous cells (Fig. 6E). In Coho salmon (*Oncorhynchus kisutch*), the presence of intracytoplasmic eosinophilic inclusions was also observed, consistent with colonies of *Chlamydia*-type bacteria. A few fish showed

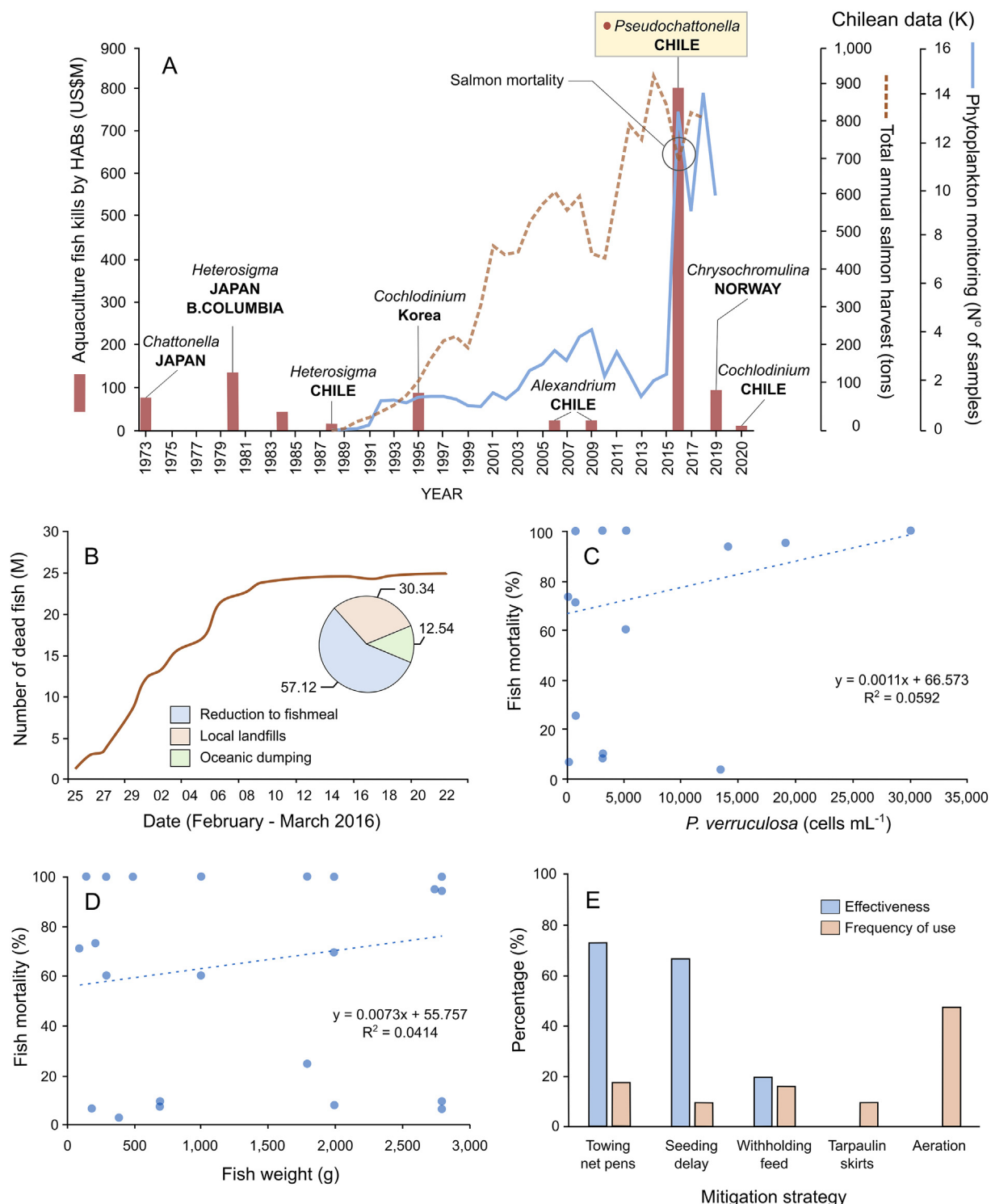


Fig. 5. A) Historical (1973–2020) worldwide aquaculture fish-kills (red bars), total annual harvest (tons) since the beginning of the Chilean salmon farming in the 1980s (orange dotted line) and total annual number of water samples for phytoplankton analysis (blue continuous line); B) Total number of dead salmon during February–March 2016 and their disposal destinations (% of total biomass); C) Relationship between *P. verruculosa* cell abundances (cells mL⁻¹) and total salmon mortality (%); D) relationship between total salmon mortality at salmon cages (%) and fish age; and E) effectiveness (%) and frequency of use (%) of mitigation strategies attempted at the salmon farms during the 2016 *P. verruculosa* fish-killing event.

subacute diffuse myocarditis and myositis (heart and red muscle, respectively), glomerulopathy and interstitial nephritis (kidney), enteritis (intestine) and granulomatous hepatitis (liver) (Fig. 6F). A detailed diagnosis by fish organ and its detection frequency (%) are tabulated in Table 2.

3.2. Laboratory studies

3.2.1. Cell morphology and life history

Cells of the Chilean *P. verruculosa* collected from natural blooms were highly variable in shape and size (Fig. 7A-F). At the initiation of the bloom (exponential growth phase) cells were usually ovoid and elliptical (Fig. 7A-B), while at the end of the bloom (stationary growth phase), pyriform, elongate and sickle-like cells were more common (Fig. 7D-F). Cell sizes ranged from 9 to 42 µm. Mucocysts at the periphery of the cell were generally smaller in the exponential growth phase (Fig. 7A) than in stationary phase (Fig. 7D). The nucleus of the cell was placed toward the fore end of the cell and generally spherical (Fig. 7C).

P. verruculosa cells decreased their size in culture (6–16 µm). Elongate and ovoid cells had two unequal flagella which emerged anteriorly, but usually only the elongated forwardly directed flagellum was visible (fl in Fig. 7G). The shorter flagellum was not clearly visible under the light microscope. Sporadically smaller cells were attached directly to the posterior end of a larger elongate cell (arrowheads in Fig. 7G). Ovoid and elliptic cells may act as gametes and fuse to form a zygote (Fig. 7H and I). The zygote can undergo nuclear division producing a much larger spherical multi-nucleate cell (Fig. 7J). The multi-nucleate cells can produce multiple daughter cells or fuse with other multi-nucleate cells giving rise to larger (<250 µm) plasmodium-like aggregates. These aggregates could be found swimming in culture and displaying numerous flagella at the periphery (Fig. 7K) or stayed non-motile for a few days. Copious flagellated offspring cells eventually were liberated through the weakened membrane of the parent cell (Fig. 7L). The use of standard fixatives such as glutaraldehyde, Lugol's iodine or formaldehyde is not recommended for cell identification because of cell deformation and rupture (Fig. 7M-O).

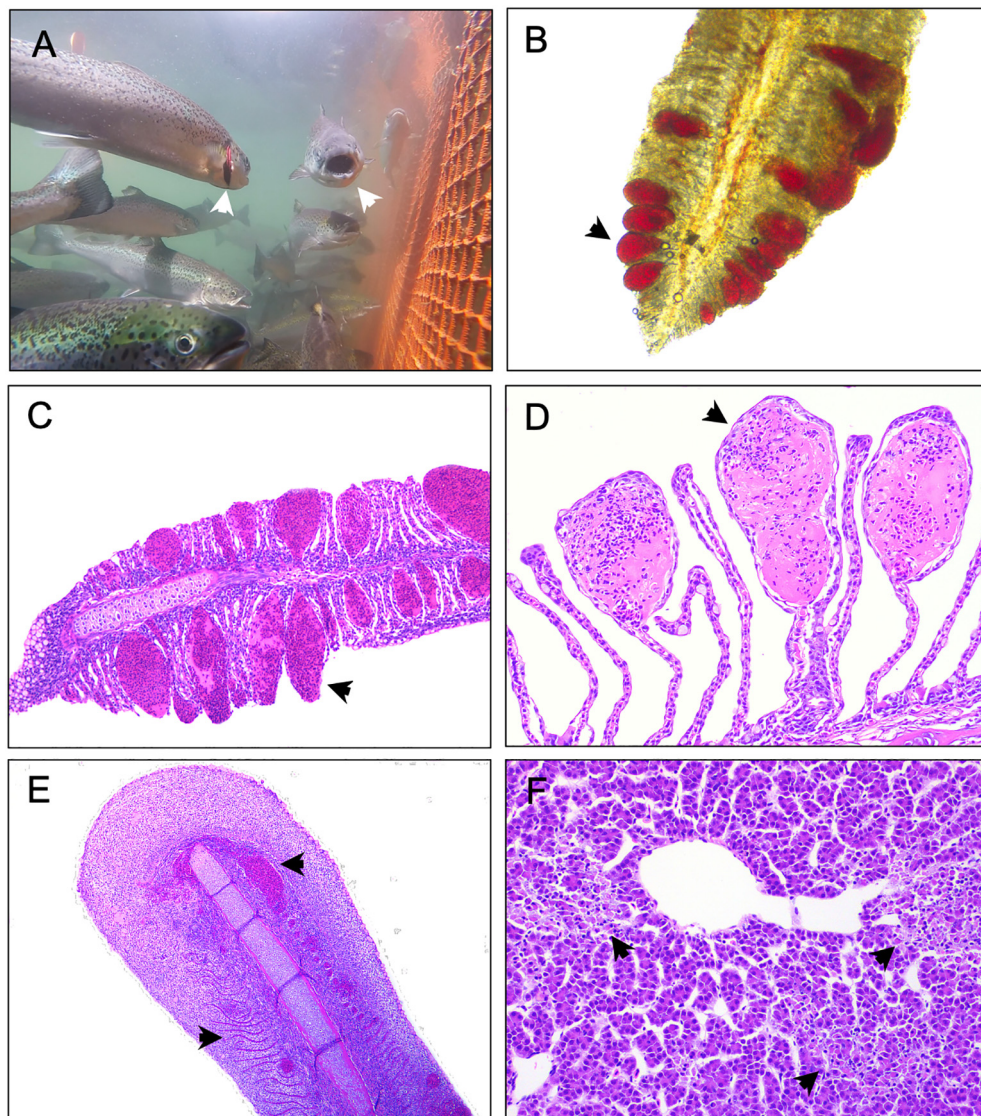


Fig. 6. *In situ* observations, whole mounts and H&E (hematoxylin and eosin) stained tissues (gill arches and liver) from moribund Atlantic salmon (*Salmo salar*) during the 2016 *P. verruculosa* event. A) Underwater picture taken at a salmon cage showing affected fish with semi-open gill operculum (left arrow) and open mouth (right arrow) evidencing respiratory distress; Histopathology showed B) Multifocal lamellar telangiectasia (whole mount); C) severe multifocal lamellar telangiectasia; D) Multifocal lamellar thrombosis showing eosinophilic material and erythrocytes within the lamellar cavities (200×); E) Branchial hyperplasia associated with spongiosis (left arrow) and hemorrhages (right arrow) (40×) and F) Multifocal hepatic necrosis with impaired hepatocyte structure (black arrows).

Table 2

Histopathological diagnosis and its frequency of occurrence (%) of affected salmon ($n=107$) from 37 salmon farms during the *P. verruculosa* bloom event at the Reloncaví Sound in summer 2016.

Organ	Diagnosis	Frequency (%)
Gill	Interlamellar hyperplasia with fusion of the secondary lamellae (moderate to severe)	50.5
	Multifocal telangiectasia (severe)	32.7
	Multifocal thrombosis (severe)	27.1
	Diffuse chondrodysplasia (moderate)	18.7
	Eosinophilic intracytoplasmic inclusions (<i>Chlamydia</i> spp. - colonies)	17.8
	Interlamellar hyperplasia with fusion of the secondary lamellae and formation of interlamellar vacuoles	16.8
	Mucous cell hyperplasia (mild to moderate)	15.9
	Diffuse Edema (moderate to severe)	14.0
	Diffuse spongiosis (moderate to severe)	13.1
	Presence of amoeboid protozoa (<i>Paramoeba perurans</i>)	10.3
Kidney	Diffuse glomerulopathy (moderate to severe)	1.9
	Diffuse interstitial nephritis (mild to moderate)	2.8
Heart	Focal to multifocal myocarditis (mild to moderate)	8.4
Red muscle	Focal to multifocal myositis (mild to moderate)	2.8
Liver	Multifocal to diffuse granulomatous hepatitis (severe)	0.9
	Multifocal hepatitis (mild to moderate)	2.8
	Diffuse hepatic steatosis (mild to moderate)	3.7
Intestine	Diffuse enteritis (mild to moderate)	0.9
Spleen	Congestion	1.9

3.2.2. *Pseudochattonella* molecular identification

Amplifications performed on 5 Chilean strains (CREAN_PV01, CREAN_PV03, CREAN_PV04, CREAN_PV05, CREAN_PV06) resulted in fragments of 475 bp and 500 bp for the LSU and *rbcL* genes, respectively. The LSU and *rbcL* trees showed that the Chilean isolates resolved into the *P. verruculosa* clade. Both *Pseudochattonella* species were not retrieved as reciprocally monophyletic in the LSU tree (Fig. S1A). The *rbcL* tree did recover the two *Pseudochattonella* species as reciprocally monophyletic (Fig. S1B).

3.2.3. *P. verruculosa* in vitro cell growth

The *in vitro* growth of five strains of *P. verruculosa* under 3 temperature treatments is shown in Fig. 8 and Table 3. Cell growth rates at different temperatures showed significant differences among treatments with a maximum of 0.75 ± 0.02 (d^{-1}) at 18°C and a minimum of 0.65 ± 0.03 (d^{-1}) at 12°C (ANOVA, $p<0.01$). Among strains, CREAN_PV03 showed the highest growth rate with 0.78 ± 0.01 (d^{-1}) and CREAN_PV05 the lowest with 0.66 ± 0.02 (d^{-1}) (ANOVA, $p<0.01$). Maximum cell density was not significantly affected by temperature (ANOVA, $p>0.01$), but there were significant differences among strains (ANOVA, $p<0.01$). CREAN_PV01 showed the highest cell densities with $566,167 \pm 13,890$ cells mL^{-1} and CREAN_PV06 the lowest with $269,083 \pm 27,722$.

3.2.4. Chlorophyll *a* cell quota

HPLC analysis of the five Chilean *Pseudochattonella* cultures showed chl *a* as the main pigment with a mean cell quota of 0.3 ± 0.11 pg cell^{-1} .

3.2.5. Superoxide anion production and fatty acid (FA) composition

Neither lysed nor intact cells of the *Pseudochattonella* CREAN_PV01 strain showed superoxide anion production while CREAN_PV03 produced low amounts of 0.12 ± 0.13 and 0.21 ± 0.19 $\text{pmol O}_2^- \text{cell}^{-1} \text{h}^{-1}$ in whole and lysed cell treatments, respectively (Fig. 10). The lipid class in the CREAN_PV01 strain was represented by $85.2 \pm 4.9\%$ phospholipids (PL), $9.1 \pm 2.9\%$ free fatty acids (FFA), $5.7 \pm 2\%$ sterols (ST), 0% triacyl-glycerols (TAG) and 0% wax esters (WE). The % of total FA of the *P. verruculosa* CREAN_PV01 strain was led by polyunsaturated fatty acid -PUFA ($69.7 \pm 1.8\%$) and only low levels of saturated fatty

acid -SFA ($15.6 \pm 0.6\%$) and monounsaturated fatty acid -MUFA ($14.7 \pm 1.4\%$). The principal FA in decreasing order of density were stearidonic (SDA, $18:4\omega 3$ -28.9%), docosahexaenoic (DHA, $22:6\omega 3$ -22.3%), myristic (MYA, $14:0$ -10.5%) and gamma-linolenic (GLA, $18:3\omega 6$ -10%) acids (Table 4).

3.2.6. *P. verruculosa* cytotoxicity

Cultured *Pseudochattonella* at cell densities between 1 and 10,000 cells mL^{-1} exposed against the gill cell line showed insignificant cytotoxicity, either as lysed or live treatments. Only the lysed cell treatment at the highest *Pseudochattonella* cell density of 100,000 cells mL^{-1} reduced gill cell viability down to 40–60% of controls (ANOVA, $p<0.05$, Fig. 11A). The highest intact live cell treatment of 100,000 cell mL^{-1} did not significantly affect gill cell viability (ANOVA, $p<0.05$, Fig. 11B). No significant effect was detected in time of exposure of lysed cells of *Pseudochattonella* against the RTgill-W1 between 1 and 6 h (ANOVA, $p<0.05$, Fig. 11A).

4. Discussion

4.1. Environmental conditions leading to the *P. verruculosa* bloom

A prolonged and extensive bloom of the dictyochophyte *P. verruculosa* occurred in south Chilean waters between January and May 2016, peaking in late February and early March. All evidence pointed to remarkable inshore and ocean water conditions in late 2015 and early 2016 because of the positive phase of the Southern Annular Mode (SAM) and a super-scale El Niño event that changed atmospheric circulation in the SE Pacific Ocean (Trainer et al., 2019). This resulted in a substantial increase in solar radiation (~30%) and the lowest summer streamflow recorded over the last 66 years, causing much warmer and more stable than usual water masses in the region (Fig. 4A). Strongly stratified water masses have been widely considered favorable to flagellate HAB events (Smayda, 2002).

The origin of the *P. verruculosa* inoculum remains undetermined, however low cell densities detected in eastern Chiloé Island waters by mid-January 2016 are considered the possible inoculum (Fig. 2). The position of the high-pressure Southeast Pacific system during summer 2016 triggered a strong wind anomaly (Fig. 4B), shifting the West Wind Drift current (WWD) (Strub et al., 2019). This atmospheric-oceanographic alteration might have enhanced a northward transport of cells from coastal Chiloé Island to Reloncaví Sound. Once the *P. verruculosa* cell inoculum reached Reloncaví Sound, the physico-chemical conditions of the water column were ideal for rapid cell growth. *In situ* data showed that the inner Sound (St. 2 and 3) with a highly stratified water column was more productive than at the mouth (St. 1 with oceanic influence). A strong halocline/thermocline on 12 January coincided with a 4 to 7 m chl *a* 'thin layer' of about $\sim 25 \mu\text{g L}^{-1}$ located between 10 and 17 m depth (Fig. 3), suggesting that the *P. verruculosa* outbreak originated and was maintained by hydrodynamic processes. Clément et al. (2016) observed even higher values of chl *a* on 7th–8th March with a maximum of $38.4 \mu\text{g L}^{-1}$ at ~10 m depth, where 93% of total phytoplankton was comprised of *P. verruculosa*. Although the CTD-F data presented in this study showed a 'thin layer' only in January and eroding in February–March, more frequent monitoring (Clément et al., 2016) indicated that thin layer formation was a dynamic and sustained process that lasted for > 2 months.

Several environmental factors might have contributed to the high cell abundance and persistence of the 2016 *P. verruculosa* bloom in the Reloncaví Sound. The advection of more saline waters from offshore zones and reduced freshwater contribution from the Puelo river have been suggested as a key factor (León-Muñoz et al., 2018). The strong halocline in January weakened and shallowed in February, which resulted in increased salinity (~28–30) in the upper surface layers of

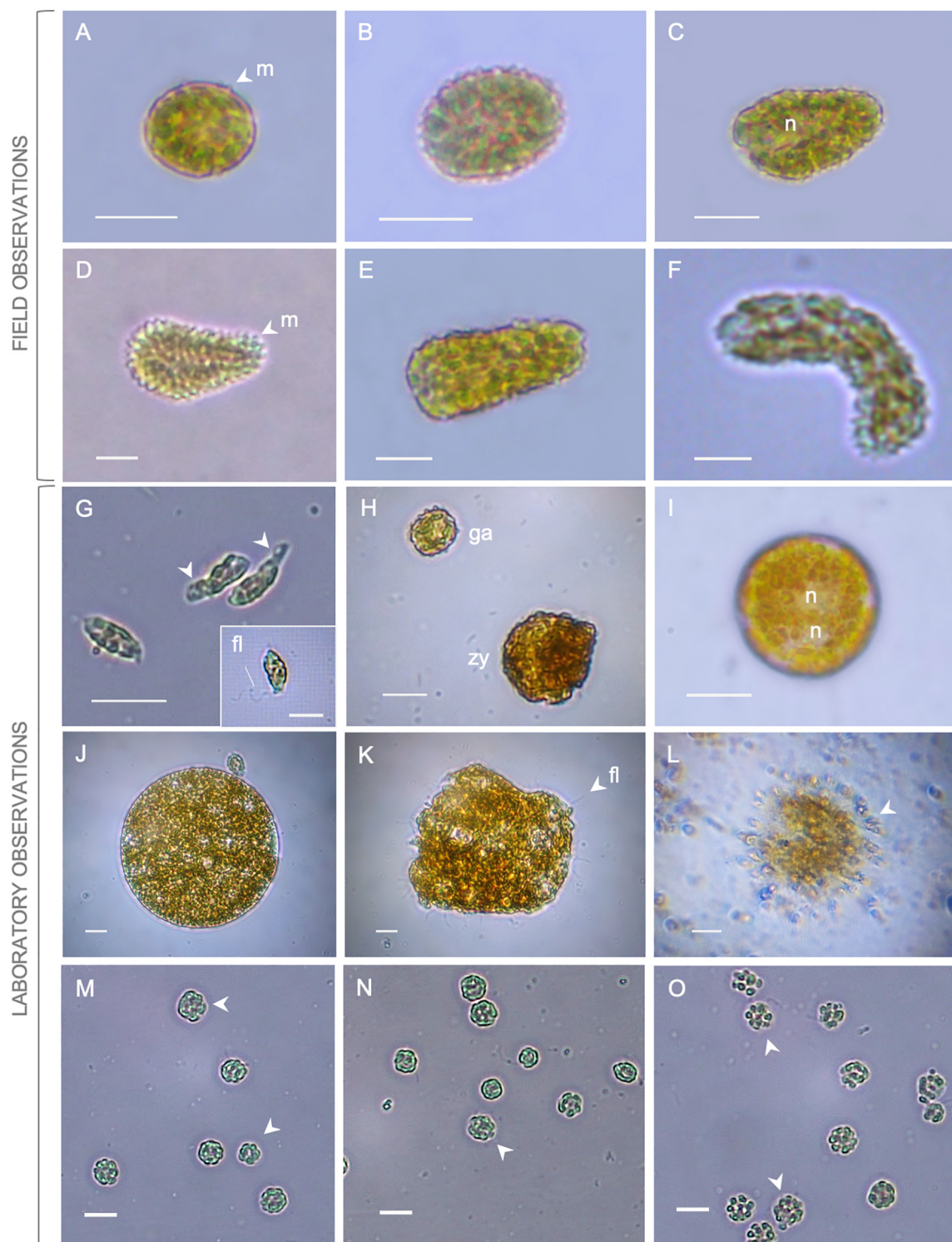


Fig. 7. (A–L) Light microscopy images of live cells of Chilean *Pseudocharonella verruculosa*. (A–F) Cells from field samples (2009 and 2016 blooms) showing variable morphologies with mucocysts at the periphery of each cell: (A) ovoid, (B) elliptic, (C–D) pyriform (E) elongate or ‘carrot’-like and (F) ‘sickle’-like shapes; (G–L) Complex life cycle stages observed in monoclonal cultures: (G) elongate cells with small oval-shape cells attached (arrowheads) and anteriorly directed flagellum (fl), (H) putative ovoid gamete (ga) and zygote (zy), (I) zygote showing nuclear division with two nuclei (n), (J) spherical multinucleate cells produced by cytokinesis, (K) plasmodium-like aggregate with multiple flagella (fl) at the periphery, (L) flagellated daughter cells released from a multinucleated cell or plasmodium-like aggregate, and (M–O) fixed cells using M) glutaraldehyde (1% final concentration), N) Lugol’s iodine (0.1% final concentration) and O) formaldehyde (0.1% final concentration). Scale bar = 10 µm.

Reloncaví Sound (Fig. 3). This shift was strongly correlated with displacement of the thin layer to the surface. In culture experiments, Mardones et al. (2019) showed that the maximum cell abundance of the *P. verruculosa* CREAN_PV01 strain was significantly higher at 30 salinity compared to lower salinity conditions. These results might

partially explain peak cell abundance close to the pycnocline in January and close to the surface during February–March in the Reloncaví Sound (Fig. 3).

Water temperature is another key factor driving microalgal bloom dynamics in shallow productive coastal waters. In January 2016, surface

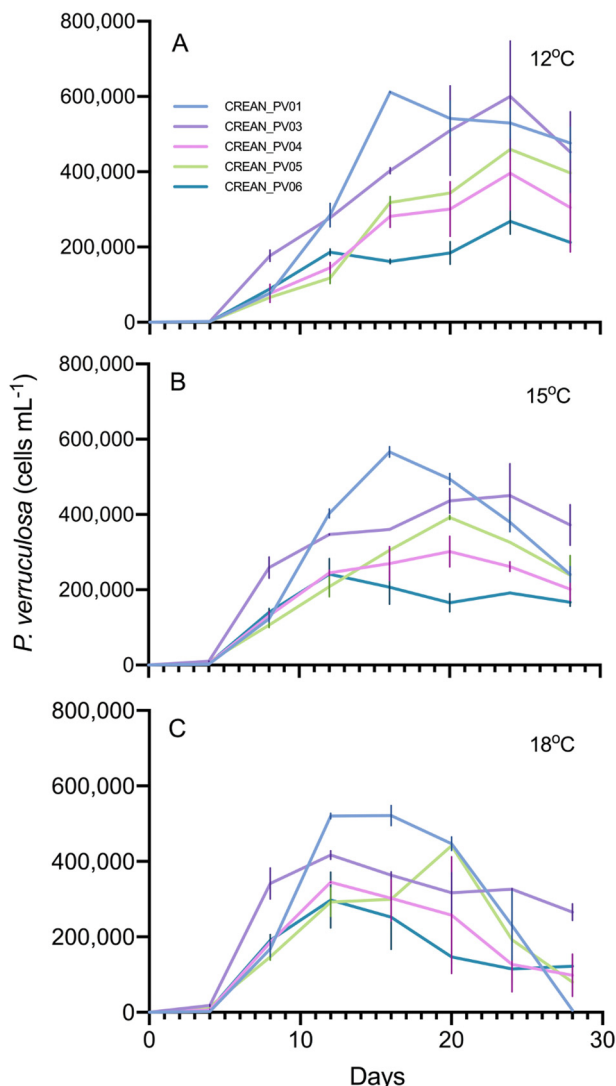


Fig. 8. Growth curves of five *P. verruculosa* strains at 3 different temperatures simulating water conditions in Reloncaví Sound in summer 2016. Bold lines represent the mean and vertical lines the standard error (SE) of cell counts from triplicate measurements.

water temperature was higher at the head of the Reloncaví Sound compared to the mouth (Fig. 3D). Warm water flow from the Puelo River produced a strong thermocline (~ $\Delta 8^{\circ}\text{C}$), which coincided with intense subsurface thin layers. The *in vitro* cell growth experiments (Fig. 8; Table 3) covered the wide range of temperatures recorded in January

Table 3

Mean, standard error (SE) and post-hoc Tukey HSD test for the maximum specific growth rate (μ_{\max}) and maximum cell density of the Chilean *P. verruculosa* strains at three different temperatures.

	μ_{\max}	SE	Tukey	Max. cell density	SE	Tukey
Strains						
CREAN_PV01	0.681	0.015	ab	566,167	13,890	d
CREAN_PV03	0.775	0.013	c	489,278	56,696	cd
CREAN_PV04	0.683	0.019	ab	347,667	33,565	ab
CREAN_PV05	0.663	0.015	a	431,292	13,026	bc
CREAN_PV06	0.698	0.014	b	269,083	27,722	a
Temperature (°C)						
12	0.647	0.027	a	467,200	46,267	a
15	0.707	0.023	b	390,542	35,081	a
18	0.746	0.022	c	404,350	24,359	a

Table 4

Fatty acid composition of the Chilean *P. verruculosa* CREAN_PV01 (as % of total fatty acids).

Fatty acid	Mean	SD
SFA		
14:0 MYA	10.5	± 0.2
15:0	0.3	± 0.0
16:0	4.2	± 0.1
17:0	0.1	± 0.0
18:0	0.4	± 0.3
24:0	0.1	± 0.0
MUFA		
16:1ω7c	1.9	± 0.2
16:1ω5c	5.0	± 0.0
16:1ω13t	1.9	± 0.0
18:1ω9c	0.2	± 0.2
18:1ω7c	3.9	± 0.1
18:1ω7t	0.4	± 0.2
18:1a	0.3	± 0.3
18:1b	0.2	± 0.2
18:1c	0.2	± 0.2
19:1b	0.1	± 0.1
20:1ω9c	0.1	± 0.0
22:1ω13c	0.1	± 0.1
22:1ω11c	0.4	± 0.0
PUFA		
18:3ω6 GLA	10.0	± 0.2
18:4ω3 SDA	28.9	± 0.3
18:2ω6	1.4	± 0.2
18:3ω3	3.5	± 0.0
20:5ω3	1.9	± 0.0
20:4ω3	0.9	± 0.0
21:5ω3	0.4	± 0.0
22:6ω3 DHA	22.3	± 0.0
22:4ω6	0.2	± 0.0
22:5ω3	0.2	± 0.1
Sum SFA	15.6	± 0.6
Sum MUFA	14.7	± 1.4
Sum PUFA	69.7	± 1.8

Abbreviations: SFA, saturated fatty acids; MUFA, monounsaturated fatty acids; PUFA, polyunsaturated fatty acids; MYA, myristic acid (14:0); GLA, gamma-linolenic acid (18:3ω6); SDA, stearidonic acid (18:4ω3); DHA, docosahexaenoic acid (22:6ω3).

2016, showing a significant effect on growth rate and maximum cell abundance by *P. verruculosa*. Lower water temperature of 12 °C produced lower growth rates but higher maximum *Pseudochattonella* cell densities compared to 18 °C. This might have enhanced high sub-surface cell aggregation at water masses of ~12 °C during summer 2016 at Reloncaví Sound. Enhanced *P. verruculosa* cell growth at low light intensity might further support this hypothesis. This study showed growth rates between 0.64 and 0.78 d^{-1} at 45 $\mu\text{mol photon m}^{-2} s^{-1}$ compared to 0.88 to 1.44 d^{-1} at 20 $\mu\text{mol photon m}^{-2} s^{-1}$ previously reported by Mardones et al. (2019). In summary, sub-surface thin layers are thought to have resulted in a positive physical-biological interaction to minimize loss rates and maintain of a dense *P. verruculosa* population, despite lower growth rates at lower water temperatures. The water retention index (WRI) MIKE 3D FM -modeled for the inner Los Lagos sea confirmed that the Reloncaví Sound has a low flushing rate of 121 to 200 days (Fig. 4C). The higher depth, with relative narrow and shallow side channels may lead to a reduced flushing rate than that of more southerly basins (mostly 0 to 60 days). Predominant winds from the south (Fig. 4B) could have further reduced surface water exchange during summer 2016, decreasing water column mixing and enhancing *P. verruculosa* cell aggregations.

4.2. Cell detection problems caused by the *P. verruculosa* life cycle

The Chilean *Pseudochattonella* exhibits a highly variable morphology and size as described for *P. verruculosa* and *P. farcimen* from other coastal areas (Jakobsen et al., 2012; Chang et al., 2014; Eckford-Soper and

[Daubjerg, 2016](#)). From natural bloom samples, Chilean *Pseudochattonella* cell shapes varied from oval or small spherical cells to long allantoid to conical shapes ([Fig. 7A-F](#)). These forms can occur with or without abundant mucocysts that create a wart-like appearance. Small spherical cells are often smooth (sparse mucocysts) with few chloroplasts whilst elongated cells have numerous mucocysts and chloroplasts. It has been suggested that morphological changes might be an indicator of growth phase or sub-optimal conditions ([Jakobsen et al., 2012](#)). Variability of shapes and sizes in *Pseudochattonella* poses a major problem for identification in monitoring programs. When mucocysts are present, as reported during the 2009 outbreak ([Mardones et al., 2012](#)), cell identification might be less difficult, compared to smooth cells which can be easily confused with other small flagellates. Moreover, *Pseudochattonella* cells are extremely fragile which renders the use of fixatives such as glutaraldehyde (1%), Lugols's iodine (0.1%) and formaldehyde (0.1%) problematic due to cell shape distortion as shown in [Figs. 7M-O](#). [MacKenzie et al. \(2011\)](#) therefore used counts of live cells on gently shaken samples that rendered cells immotile sufficiently for cell counts to be performed. In our work, after both gentle and vigorous shaking, *Pseudochattonella* cell swimming was rapidly reestablished (~2 min).

Following isolation of Chilean *P. verruculosa* cells from 2016 into culture (1 strain) and 2019 (4 strains), all cultures exhibited a polymorphic life history ([Fig. 7](#)). As proposed by [Chang et al. \(2014\)](#), two gametes combine to form a zygote ([Fig. 7H](#)) which produces a multinucleated cell ([Fig. 7J](#)). These large multi-nucleated cells then can fuse to produce a 'massive' plasmodium-like aggregate ([Fig. 7K](#)). Ultimately, solitary small flagellated offspring cells (~4 µm) are liberated by disintegration of the large parent cell membrane ([Fig. 7L](#)). Alternatively, single cells can also undergo asexual division to produce smaller daughter cells (~4 µm) ([Fig. 7G](#)). [Fig. 7](#) shows differences between field samples and laboratory cultures of the Chilean *P. verruculosa* using light microscopy. We conclude that it is likely that monitoring programs overlooked unknown stages of *P. verruculosa*, and hence underestimated cell counts that were between 7000 and 20,000 cells mL⁻¹ in 2016. This is supported by chl *a* cell quotas estimated by HPLC from five *P. verruculosa* strains compared against *in situ* chl *a* measurements at Reloncaví Sound in 2016 ([Fig. 9](#)). Based on estimates of 0.3 ± 0.11 pg chl-*a* per cell (five strains), and assuming that thin layers were entirely made up of *P. verruculosa* as reported by [Clément et al. \(2016\)](#), *in situ* chl-*a* measurements of 25 µg L⁻¹ corresponded to ~320,000 cells mL⁻¹ (averaged cell size). Higher *in situ* chl *a* values of 38.4 µg L⁻¹ reported by [Clément et al. \(2016\)](#) might have corresponded to ~490,000 cells mL⁻¹. These values are more in line with those obtained from *in vitro* cultures ([Table 3](#); [Fig. 8](#)) and cytotoxicity against the RTgill-W1 cell line measured at 100,000 cells mL⁻¹ ([Fig. 11](#)). *P. verruculosa* is highly tolerant to elevated pH, with growth ending at pH 9.1 ([Eckford-Soper and Daubjerg, 2016](#)), which might support the hypothesis that this species can maintain high cell densities during high pH generated due to photosynthetic activity. Potential underestimation of cell counts of *Pseudochattonella* highlights the need for new tools for detection.

4.3. *P. verruculosa* identification by molecular markers

Phylogenetic reconstruction using both LSU and *rbcL* genes resolved that the *Pseudochattonella* strains from southern Chile in 2016 and 2019 correspond to *P. verruculosa* ([Fig. S1](#)). Since the first attempts of genetic characterization of *Pseudochattonella*, the LSU rDNA and SSU sequences have been shown valuable for species delineation ([Edvardsen et al., 2007](#)). This was confirmed by [Riisberg and Edvardsen \(2008\)](#) in a detailed examination of several genes (LSU, *rbcL* and *cox1*) using a number *Pseudochattonella* strains. Interestingly, low genetic distance among strains suggest that *P. farcimen* and *P. verruculosa* are closely related taxa ([Riisberg and Edvardsen, 2008](#)). So far, all *Pseudochattonella* isolates from the southern Chilean coast correspond to *P. verruculosa* ([Paredes et al., 2016](#); this study). Based on sequences of mitochondrial encoded COI ([Chang et al., 2014](#)), *Pseudochattonella* isolated from New

Zealand (Wellington Harbour) has been hypothesized to be derived from hybridization between *P. verruculosa* and *P. farcimen*. Further genetic studies are required to support this hypothesis as the sequences by [Chang et al. \(2014\)](#) are not publicly available.

The isolation of more strains from other localities are needed to discard the existence of *P. farcimen* in Chilean waters. The first report of *P. verruculosa* (as *Chattonella verruculosa*) was from Japan in 1989 ([Yamaguchi et al., 1997](#)), but since then progressively this species has been identified as the responsible of fish-kills in Germany ([Riisberg and Edvardsen, 2008](#)), New Zealand ([MacKenzie et al., 2011](#)) and Chile ([Mardones et al., 2019](#)). The Chilean *P. verruculosa* strains clustered along with isolates from Germany, Japan and New Zealand with negligible genetic distance despite their distant geographic origins. Further studies using a variety of genetic markers may help to reveal whether *P. verruculosa* was introduced in recent times or represents a native species in southern Chile. Due to the close genetic relationship among worldwide *Pseudochattonella* isolates, existing molecular markers ([Riisberg and Edvardsen, 2008](#)) could be used to improve accuracy in *P. verruculosa* cell detection for an effective early-warning system in Chile.

4.4. Fish-killing mechanism of *P. verruculosa*

Finfish in intensive aquaculture operations are extremely vulnerable to FKA blooms, with a diversity of physiological mechanisms that can act individually or in combination, including: 1) physical gill damage; 2) 'ichthyotoxins'; 3) blood hypoxia from environmental oxygen reduction; and 4) gill lesions and gas bubble trauma due to extreme oxygen supersaturation from algal photosynthesis ([Lutz, 1995](#)). Neither fish blood hypoxia nor bubble trauma are considered as the mortality mechanism involved in the Chilean salmon mortality in 2016. Dissolved oxygen was permanently above 60% and below 150% saturation at the 3 sampling sites between January and March ([Fig. 3](#)). Salmon farmers also reported DO > 3.5 mg L⁻¹, defined as a critical oxygen threshold (*P_{crit}*) for *Salmo salar* at 14 °C by [Barnes et al. \(2011\)](#). Moribund fish were observed swimming on the surface with loss of balance and evident respiratory distress with semi-open operculi ([Fig. 6A](#)). Histological inspection of fish tissues showed pathologies that might have been because of a failure of osmoregulation and hypoxia as a result of severe gill damage. Most of the examined fish showed interlamellar hyperplasia with fusion of the secondary lamellae (moderate to severe), multifocal telangiectasia (severe) and multifocal thrombosis (severe) ([Table 2](#)). Gill hyperplasia is a cell growth disorder that might be explained by previous exposition to noxious microalgae, as well as infectious agents such as amoebas (*Paramoeba perurans*) and/or *Chlamydia*-type bacteria,

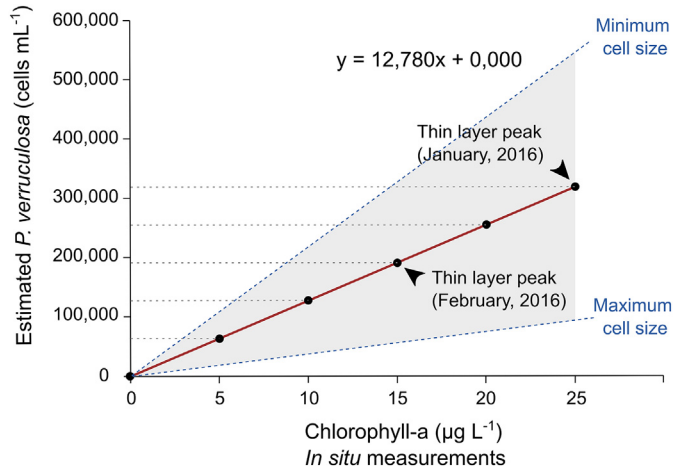


Fig. 9. Estimation of *P. verruculosa* cell abundance based on *in vitro* HPLC chl *a* cell content (0.3 ± 0.11 pg) of five strains and *in situ* chl *a* measurements during the 2016 bloom event at the Reloncaví Sound.

which together constitutes the so-called "Complex Gill Disease (CGD)" (Apablaza et al., 2017; Herrero et al., 2018). High cell densities of the diatoms *Leptocylindrus danicus* and *L. minimus* (max. 3000–9000 cells mL^{-1}) detected in Reloncaví Sound previous to the *P. verruculosa* bloom, as well as the presence of *Tenacibaculum maritimum* in salmon gill tissue (Apablaza et al., 2017), might have contributed this pathology. In addition, it has been reported that decrease in rainfall, and increased water temperature and salinity are environmental triggers for infections by parasites such as *Paramoeba perurans*. Conversely, gill telangiectasia and thrombosis are circulatory disorders that might have been caused by a cytotoxic substance released during the *P. verruculosa* bloom. Other diagnoses such as myocarditis and myositis in heart and red muscle correspond to a viral disease produced by *Piscine orthoreovirus*, and inflammatory changes such as granulomatous hepatitis, nephritis and enteritis can be explained by Salmonid Rickettsial Septicaemia (SRS) produced by *Piscirickettsia salmonis* and/or Bacterial Kidney Disease (BKD) produced by *Renibacterium salmoninarum*. Only a few cases showed necrosis in liver tissue consistent with exposure to nephro- and hepato-toxins as observed by MacKenzie et al. (2011) during a *P. verruculosa* outbreak in New Zealand. These pathologies, however, can also be due to viral and bacterial infections caused by fish gill damage with subsequent systemic hypoxia and liver ischemia.

Pseudochattonella ichthyotoxic potency remains poorly understood. Montes et al. (2018) using phytoplankton monitoring data projected that Chilean *P. verruculosa* is highly toxic, with a threshold of ~1 cell mL^{-1} to produce abnormal fish behavior. In the present study, dense *in vitro* cultures of *P. verruculosa* were weakly toxic to the RTgill-W1 gill cell line. Only lysed cell densities of 100,000 cell mL^{-1} reduced gill cell viability in 40–50% and no cytotoxic effect was observed using live cells at the same cell density (Fig. 11). Similar results were previously observed in salmon smolts (*Salmo salar*) and cod (*Gadus morhua*) where only extreme cell *Pseudochattonella* densities (10,000–30,000 cells mL^{-1}) caused reduced performance and functioning of the gills (Skjelbred et al., 2011).

The following hypotheses are offered to explain these inconsistencies. The first is that *Pseudochattonella* may lose cytotoxic activity once cultured in laboratory conditions, as suggested by Andersen et al. (2015). Microalgae in mono-clonal conditions would not need to compete against other phytoplankton, hence reducing the ability to produce toxic allelopathic compounds. Jakobsen et al. (2012), however, failed to detect any chemically mediated allelopathic interaction between *P. farcimen* and the diatoms *Chaetoceros diadema* and *C. decipiens* and the dinoflagellate *Heterocapsa triquetra* in mixed growth experiments. Nevertheless, it would be valuable to evaluate allelopathic capacity of *Pseudochattonella* against different co-occurring microalgae species. A second hypothesis is that *Pseudochattonella* is indeed weakly toxic and that only extremely elevated cell densities (>10,000 cells mL^{-1}) can be deleterious for fish farming. But then, how did the 2016 mortality happen if cell densities did not exceed 10,000 cells mL^{-1} ? A plausible explanation is that monitoring programs underestimated true *P. verruculosa* cell densities. High *in situ* chl a values in 2016, high biomass under culture conditions and numerous unknown growth stages are discussed in detail in Section 4.2. Another contributing factor may have been damage to fish gills from the preceding diatom bloom that hence increased the fish sensitivity to *Pseudochattonella*.

PUFA in the free fatty acid (FFA) form can be a known source of ichthyotoxicity (Dorantes-Aranda et al., 2015). PUFAAs can be readily oxidized due to their high degree of unsaturation (Else and Krafte, 2015; Guichardant et al., 2011), and the oxidized form can then be lethal. Chilean *P. verruculosa* cells contained high proportions of stearidonic (SDA, 18:4 ω 3–28.9%), docosahexaenoic (DHA, 22:6 ω 3–22.3%), myristic (MYA, 14:0–10.5%) and gamma-linolenic (GLA, 18:3 ω 6–10%) acids (Table 5). It has been shown that SDA increases the toxicity of doxorubicin (DOX) in human PCa cells (Mansour et al., 2018), γ -Linolenic acid is cytotoxic to 36B10 rat astrocytoma cells (Vartak et al., 1998) and DHA is cytotoxic to RTgill-W1 (Mardones et al., 2015). In most

microalgae, the highest proportions of DHA are obtained at high irradiance (i.e., summer 2016) (Thomson et al., 1990; Brown et al., 1993). Considering that PUFAAs represented 1×10^{-5} ppm *Pseudochattonella* cell $^{-1}$ and ~10% corresponded to FFA forms, we estimate that 100,000 cell mL^{-1} of *P. verruculosa* would correspond to 0.2 ppm of FFA. This value is low compared with an estimated 2.7 ppm as LC50 for eicosapentaenoic acid (EPA) in the FFA form for damselfish (Marshall et al., 2003). Yet, several multifactorial considerations have to be considered. Reactive oxygen species (ROS), involving a synergistic reaction with FFA has been suggested a primary ichthyotoxic mechanism (Dorantes-Aranda et al., 2015). Marshall et al. (2003) predicted that only 0.2 ppm EPA in the presence of ROS (as superoxide anion) provided an LT50 of 83 min for damselfish. Thus, small amounts of FFA can become highly toxic to fish in the presence of ROS. This value of 0.2 ppm of FFA at high *P. verruculosa* cell densities (>100,000 cells mL^{-1}) might then be considered harmful to fish, but Chilean *Pseudochattonella* was shown to be an extremely low ROS producer (Fig. 10). Future efforts are needed to assess the role of alternative sources of ROS in the surrounding aquatic environment that could potentially interact with FFAs. Other possible sources include: 1) ubiquitous ROS in natural waters (10^{-18} – 10^{-6} mol L^{-1}) (Díaz and Plummer, 2018); 2) radiolysis and photolysis of water molecules (high radiation levels in summer 2016); 3) positive relationship between light levels and algal ROS production (Marshall et al., 2002); 4) production by other microalgae and bacterial populations (Díaz and Plummer, 2018) and 5) water oxygen supersaturation due to high phytoplankton photosynthesis and/or local oxygen-airlifting systems from salmon farms. The latter, could also potentially contribute to *Pseudochattonella* cell rupture and vertical 'thin layer' mixing around salmon farms as observed in 2016 (Fig. 1E).

Another key research topic is the persistence of polyunsaturated aldehydes (PUAs) naturally released by microalgae (Wichard et al., 2005; Fontana et al., 2007) and/or from synergistic reaction between ROS and PUFA (FFA form) after cell rupture. It has been evidenced that PUAs can persist in seawater from 60 to 200 h depending on water temperature (Bartual and Ortega, 2013), with potentially serious implications for fish gill damage. This fact suggest that PUAs and other toxic lipid derivatives can become highly concentrated in the water column during high biomass *Pseudochattonella* outbreaks in a potential scenario of higher cell growth rates versus PUAs degradation rates. Sounds and fjords with extremely low flushing rate, as shown for Reloncaví Sound in this study, could exacerbate the persistence of ichthyotoxic compounds produced by FKA species.

4.5. Salmon mortality and mitigation strategies

The 2016 *P. verruculosa* bloom event produced US\$800 M in losses for the Chilean salmon industry, and it is now considered the largest mortality of farmed finfish ever caused by a HAB (Hallegraeff et al., 2017; Fig. 5A). During late February and early March, the massive *P. verruculosa* bloom killed a record amount of ca. 40,000 tons of salmon, equivalent to ca. 25 million fish in only 2 weeks (Fig. 5B). The magnitude of mortality was so high, that the fish carcasses could not be processed as fishmeal (57%) or disposed of in landfills (30%), but led to a request for permission to dump salmon (13%) into the ocean at 75 nautical miles (NM) off Chiloé Island (Fig. 5B). This governmental authorization was later highly criticized (Armijo et al., 2020). The authorization was granted without having a baseline of the oceanographic conditions of the coastal zone and without knowing the potential effects of such a large amount of organic matter and extra-chemicals on marine life. After that event, Chilean government authorities changed waste control strategies by increasing inspection on the managing processes by the salmon industry.

Harmful algal blooms are a societal concept, based on whether its occurrence has harmful effects (Smayda, 1997). Unlike phycotoxin-producing HAB species in Chile (i.e., *Alexandrium*, *Dinophysis* and

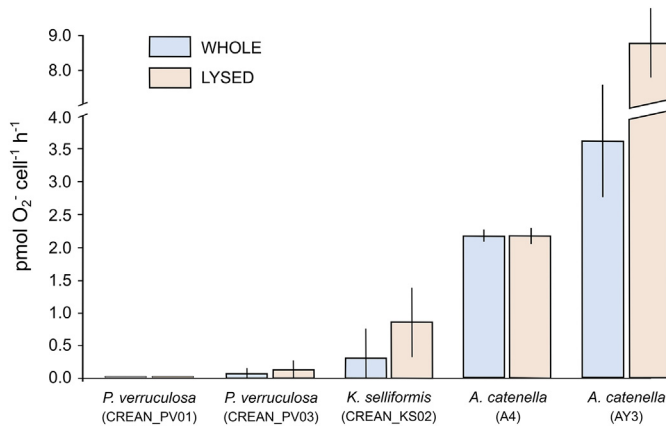


Fig. 10. Production of superoxide radical O_2^{\bullet} by two Chilean *P. verruculosa* strains (CREAN_PV01 and CREAN_PV03) from whole (blue bars) and lysed cells (orange bars) treatments. Superoxide production from the Chilean fish-killing species *Karenia selliformis* (Mardones et al., 2020) and *Alexandrium catenella* (Mardones et al., 2015) have been added for comparison.

Pseudo-nitzschia), fish-killing algae are largely undefined in terms of the extent to which they can cause harmful events. For Chilean *P. verruculosa*, an extremely low threshold value $< 1 \text{ cell mL}^{-1}$ has been suggested based on correlation with anomalous salmon behavior (Montes et al., 2018). In this study, a survey on 37 out of total salmon farms affected ($n=45$) during the 2016 bloom event showed no significant correlation between *P. verruculosa* cell abundance (quantified by salmon farmers) and the magnitude of fish mortality ($R^2=0.06$; Fig. 5C). In six cases, 10 to 100% fish mortality was related to $<3000 \text{ cells mL}^{-1}$, and in a particular case $\sim 13,000 \text{ cells mL}^{-1}$ produced 5% fish mortality. Such discrepancies have been documented from other coastal areas, where a certain HAB species can kill fish in a particular region, but not in another (Rensel and Whyte, 2003). It has also been suggested that adult fish ($>2 \text{ kg}$) can be more sensitive to *Pseudochattonella* cells than juvenile fish (Backe-Hansen et al., 2001) due to larger gills; however, this study showed no significant difference in salmon mortality related to fish age among 37 salmon farms surveyed during the 2016 *P. verruculosa* outbreak ($R^2=0.04$; Fig. 5D).

Mitigation of HABs at fish farms is generally not a urgency until a major fish-killing bloom or sequence of toxic outbreaks occur. Despite phytoplankton monitoring increasing from ~2200 water samples per year (average between 2000 and 2015) to ca. 14,000 in 2016 (Fig. 5A), the 2016 salmon mortality could not be avoided. Several mitigation methods were attempted at salmon farms during the HAB contingency in 2016, but only a few showed some degree of effectiveness (Fig. 5E).

Aeration (*i.e.*, airlift upwelling and bubble curtains) is extensively performed in marine fish farms for mitigating the deleterious effects of HABs that produce water anoxia or hypoxia (Fig. 1E) (Rensel and Whyte, 2003). This method is primarily used in Washington State and British Columbia to avoid fish-kills from *Heterosigma* (Haigh and Esenkulova, 2014), and is occasionally used in South Korea for *Margalefidinium* (Kim, 2012). In 2016, this method was the most common among those used by Chilean farmers but proved the least effective (Figs. 5E). The purpose of airlift-upwelling is to interchange the microalgal-dense surface water with microalgae-free deep water; However, in Chile the depth distribution of *P. verruculosa* was not closely tracked, which might have inadvertently resulted in airlifted water that contained dense *Pseudochattonella* 'thin layers' and that possibly lysed cells as well.

In 2016, the airlift upwelling with aeration was alternatively used with perimeter tarpaulin skirts as a companion method. A benefit of this method is that the upwelled water is less prone to be 'polluted' by nearby surface water with elevated microalgal densities, but a disadvantage is that skirts without aeration might result in low oxygen levels (Stien et al., 2012). This method was also unsuccessful against the Chilean *P. verruculosa* bloom (Figs. 5E). Similar negative results were observed against *Margalefidinium* sp. outbreaks in BC Canada, apparently because this dinoflagellate can vertically migrate up to 25 m depth (Whyte et al., 2001). A more effective mitigation method was withholding feed (Fig. 5E) but this is only recommended for short-term events. Over long periods, as during the Chilean event (>4 weeks), withholding feed can increase physiological stress (*i.e.*, reduced liver glycogen, weight loss) and proneness to chronic infections such as BKD (Rensel and Whyte, 2003). By contrast, besides delaying seeding of juvenile fish during the algal bloom and net pen towing from the affected area to a safe refuge area were the most effective mitigation measures implemented (Figs. 5E). The latter method, however, not widely practiced since it risks fish escape due to structural damage to facilities, and increases fish mortality from stress and crowding. Net pens towing has also been practiced during blooms of *H. akashiwo* in Washington State and BC Canada (Whyte, 1997; Horner et al., 1997), *K. mikimotoi* and *Chrysochromulina polylepis* in Norway, and *Chattonella* in the Seto Inland Sea of Japan and Hong Kong (Anderson et al., 2001).

The multi-factorial complexity behind HABs hinders the improvement of successful mitigation methods and monitoring; however, the implementation of selected fish farming action plans has potential benefits. Here, there are some recommendation:

- Careful site selection considering carrying capacity, depth, flushing characteristics and history of HAB in the area
- Conduct routine monitoring cell counts and train staff to recognize different life stages of FKA species

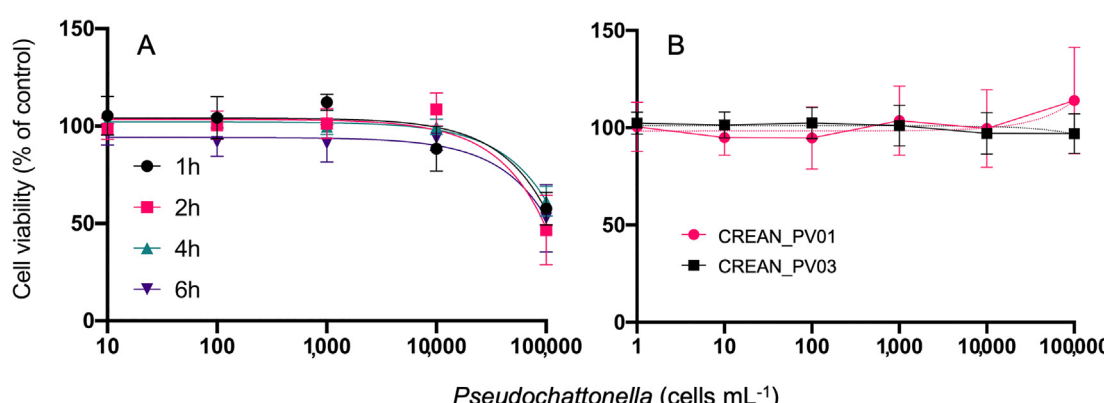


Fig. 11. *P. verruculosa* cytotoxicity potency against the RTgill-W1 cell line. A) Concentration (10 to 100,000 cell mL^{-1}) and time (1 to 6 h)-dependent toxicity of lysed cells of the CREAN_PV01 strain; and B) Whole cell treatment (1 to 100,000 cell mL^{-1}) of two strains (CREAN_PV01 and CREAN_PV03) after 2 h exposure. Symbols represent the mean and error bars the standard deviation of cell viability from quadruplicate measurements.

- Implement molecular tools and bio-optical tools (HPLC pigment analysis, remote sensing) for enhanced FKA species tracking
- Closely track vertical (thin layers) and horizontal (patches) ichthyotoxic cell aggregations by discrete water sampling (i.e., Niskin bottles) and/or *in situ* vertical fluorescence profiles
- Develop a multi-stage and flexible bloom response plan to deal with different types of HABs
- Become familiar with behavioral and physiological signs that fish are stressed by HABs
- Begin pre-emptive harvesting and stop feeding fish as blooms approach
- Avoid handling and other activities during bloom to reduce stress on fish
- Evaluate local conditions and options such as safe haven locations to tow net cages
- Rapidly proceed with pre-designated fish mortality recycling or disposal plans

It is hoped that these suggestions might contribute toward prevention and mitigation of massive farmed-fish mortalities due to ongoing increasing fish-killing algal blooms in southern Chile.

4.6. Lessons from the 2016 *P. verruculosa* bloom

A significant gap exists in our ability to manage fish killing algal (FKA) blooms in southern Chile. We point to major discrepancies between estimated *Pseudocharonella* ichthyotoxic potency using phytoplankton monitoring data (Montes et al., 2018) and *in vitro* observations. Our analysis suggests that historical monitoring has underestimated *P. verruculosa* cell densities during bloom events (especially in 2016). Arguments to support this claim, include: 1) The complex *P. verruculosa* life cycle with growth stages overlooked in monitoring programs; 2) fragility and distortion of cells when using fixatives (live cell counts are not recommended); 3) high chl *a* concentrations from nearly mono-specific populations, consistent with higher *Pseudocharonella* cell densities than what were measured; 4) maximum cell densities of 5 *P. verruculosa* strains (390,000 and 467,000 cells mL⁻¹) achieved in culture conditions were far higher than cell counts during the 2016 bloom event (max. ~10,000 cells mL⁻¹); and 5) *in vitro* *P. verruculosa* cytotoxicity against the RTgill-W1 cell line was only detectable at lysed cell concentrations as high as 100,000 cells mL⁻¹. Moreover, lipid class analysis on *P. verruculosa* CREAN_PV01 strain showed that only high cell densities (>100,000 cells mL⁻¹) can be considered toxic to fish under oxidative environments (0.2 ppm in the free fatty acid form).

An essentially similar result, of not being able to reproduce the fish-killing activity by natural *P. farcimen* blooms in Danish waters when brought into culture was reported by Andersen et al. (2015). Significant strain differences in ichthyotoxic activity between *P. verruculosa* strains from Norway and Japan were emphasized by Skjelbred et al. (2011). Performing the gill assay on water samples freshly returned to the lab may be one way to confirm ichthyotoxicity in nature and define the environmental drivers and strain variation that influence it. The use of molecular-based methods is recommended for effective local *Pseudocharonella* early warnings.

Supplementary data to this article can be found online at <https://doi.org/10.1016/j.scitotenv.2020.144383>.

CRediT authorship contribution statement

Jorge I. Mardones: Conceptualization, Writing – original draft, Data curation, Methodology, Formal analysis, Investigation, Project administration, Writing – review & editing. **Javier Paredes:** Data curation, Formal analysis, Methodology. **Marcos Godoy:** Data curation, Formal analysis, Methodology, Investigation, Writing – review & editing. **Rudy Suarez:** Data curation, Formal analysis, Methodology. **Luis Norambuena:** Formal

analysis, Methodology. **Valentina Vargas:** Data curation, Formal analysis. **Gonzalo Fuenzalida:** Data curation, Formal analysis. **Elias Pinilla:** Data curation, Formal analysis. **Osvaldo Artal:** Data curation, Formal analysis. **Ximena Rojas:** Data curation, Formal analysis. **Juan José Dorantes-Aranda:** Data curation, Formal analysis. **Kim J. Lee Chang:** Data curation, Formal analysis. **Donald M. Anderson:** Visualization, Writing – review & editing. **Gustaf M. Hallegraeff:** Visualization, Writing – review & editing.

Declaration of competing interest

The authors declare that they have no known competing financial interests or personal relationships that could have appeared to influence the work reported in this paper.

Acknowledgements

The authors thank colleagues from the CREAN group for laboratory and field work. Funding was provided by the Instituto de Fomento Pesquero (IFOP) (Grants MR656-129 and CORFO 480-018). Support for DMA was provided through the Woods Hole Center for Oceans and Human Health (National Science Foundation grant OCE-1840381 and National Institutes of Health grants NIEHS-1P01-ES028938-01).

References

- Alves-de-Souza, C., Iriarte, J.I., Mardones, J.I., 2019. Interannual variability of *Dinophysis acuminata* and *Protoceratium reticulatum* in a Chilean fjord: insights from the realized niche analysis. *Toxins* 11, 1–23.
- Andersen, N.G., Hansen, P.J., Engell-Sørensen, K., Nørremark, L.H., Andersen, P., Lorenzen, E., Lorenzen, N., 2015. Ichthyotoxicity of the microalgae *Pseudocharonella farcimen* under laboratory and field conditions in Danish waters. *Dis. Aquat. Org.* 116, 165–172.
- Anderson, D.M., Andersen, P., Bricelj, V.M., Cullen, J.J., Rensel, J.E., 2001. Monitoring and management strategies for harmful algal blooms in coastal waters. APEC #201-MR-01.1. Asia Pacific Economic Program, Singapore, and Intergovernmental Oceanographic Commission Technical Series No. 59, Paris (264 p.).
- Anisimova, M., Gascuel, O., 2006. Approximate likelihood-ratio test for branches: a fast, accurate, and powerful alternative. *Syst. Biol.* 55, 539–552.
- Apablaza, P., Frisch, K., Brevik, Ø.J., Småge, S.B., Vallestad, C., Duesund, H., Mendoza, J., Nylund, A., 2017. Primary isolation and characterization of *Tenacibaculum maritimum* from Chilean Atlantic salmon mortalities associated with a *Pseudocharonella* spp. algal bloom. *J. Aquat. Anim. Health* 29 (3), 143–149.
- Armijo, J., Oerder, V., Auger, P.-A., Bravo, A., Molina, E., 2020. The 2016 red tide crisis in southern Chile: possible influence of the mass oceanic dumping of dead salmon. *Mar. Pollut. Bull.* 150, 110603.
- Avendaño-Herrera, R., 2018. Proper antibiotics use in the Chilean salmon industry: policy and technology bottlenecks. *Aquaculture* 495, 803–805.
- Baba, T., Momoyama, K., Hiraoka, M., 1995. A harmful flagellate plankton increased in Tokuyama Bay. *Bull. Yamaguchi Prefect. Naikai Fish. Exp. Stn.* 24, 121–122.
- Backe-Hansen, P., Dahl, E., Danielssen, D.S., 2001. On the bloom of the *Chattonella* in the North Sea/Skagerrak in April–May 1998. In: Hallegraeff, G.M., Blackburn, S.I., Bolch, C.J.S., Lewis, R. (Eds.), Harmful Algal Blooms 2000. Intergovernmental Oceanographic Commission of UNESCO, Paris, pp. 78–81.
- Barnes, R., King, H., Carter, C.G., 2011. Hypoxia tolerance and oxygen regulation in Atlantic salmon, *Salmo salar* from a Tasmanian population. *Aquaculture* 318, 397–401.
- Bartual, A., Ortega, M.J., 2013. Temperature differentially affects the persistence of polyunsaturated aldehydes in seawater. *Environ. Chem.* 10, 403–408.
- Brown, M.R., Dunstan, G.A., Jeffrey, S.W., Volkman, J.K., Barrett, S.M., LeRoi, J.M., 1993. The influence of irradiance on the biochemical composition of the prymnesiophyte *Isochrysis* sp. (Clone T-ISO). *J. Phycol.* 29, 601–612.
- Chang, F.H., Zeldis, J., Gall, M., Hall, J., 2003. Seasonal and spatial variation of phytoplankton assemblages, biomass and cell size from spring to summer across the Northeastern New Zealand continental shelf. *J. Plankton Res.* 35, 737–758.
- Chang, F.H., Zeldis, J., McVeagh, M., Gall, M., 2014. Molecular phylogeny, pigment composition, toxicology and life history of *Pseudocharonella* cf. *verruculosa* (class Dictyochophyceae) from Wellington Harbour, New Zealand. *Harmful Algae* 34, 42–55.
- Clément, A., Lincoquero, L., Saldivia, M., Brito, C.G., Muñoz, F., Fernández, C., Pérez, F., Maluje, C.P., Correa, N., Moncada, V., Contreras, G., 2016. Exceptional summer conditions and HABs of *Pseudocharonella* in southern Chile create record impacts on salmon farms. *Harmful Algal News* 53, 1–3.
- Daugbjerg, N., Henriksen, P., 2001. Pigment composition and rbcL sequence data from the silicoflagellate *Dictyota speculum*: a heterokont alga with pigments similar to some haptophytes. *J. Phycol.* 37, 1110–1120.
- Dayeh, V.R., Schirmer, K., Lee, L.E.J., Bols, N.C., 2005. Rainbow trout gill cell line microplate cytotoxicity test. In: Blaise, C., Férid, J.F. (Eds.), Small-Scale Fresh-water Toxicity Investigations. Springer, The Netherlands, pp. 473–503.

- Díaz, J.M., Plummer, S., 2018. Production of extracellular reactive oxygen species by phytoplankton: past and future direction. *J. Plankton Res.* 40 (6), 655–666.
- Dorantes-Aranda, J.J., Waite, T.D., Godratt, A., Rose, A., Tovar, C.D., Woods, G.M., Hallegraeff, G.M., 2011. Novel application of a fish gill cell line assay to assess ichthyotoxicity of harmful marine microalgae. *Harmful Algae* 10, 366–373.
- Dorantes-Aranda, J.J., Seger, A., Mardones, J.I., Nichols, P.D., Hallegraeff, G.M., 2015. Progress in understanding algal bloom-mediated fish kills: the role of superoxide radicals, phycotoxins and fatty acids. *PLoS One* 10 (7), e013549.
- Eckford-Soper, L., Daugbjerg, N., 2016. The ichthyotoxic genus *Pseudochattonella* (Dictyochophyceae): distribution, toxicity, enumeration, ecological impact, succession and life history – A review. *Harmful Algae* 58, 51–58.
- Edvardsen, B., Shalchian-Tabrizi, K., Jakobsen, K.S., Medlin, L.K., Dahl, E., Brubak, S., Paasche, E., 2003. Genetic variability and molecular phylogeny of *Dinophysis* species (Dinophyceae) from Norwegian waters inferred from single cell analyses of rDNA. *J. Phycol.* 39, 395–408.
- Edvardsen, B., Eikrem, W., Shalchian-Tabrizi, K., Riisberg, I., Johnsen, G., Naustvoll, L., Throndsen, J., 2007. *Verrucophora farcimen* gen. et sp. nov. (Dictyochophyceae, Heterokonta) – a bloom-forming ichthyotoxic flagellate from the Skagerrak, Norway. *J. Phycol.* 43, 1054–1070.
- Eikrem, W., Edvardsen, B., Throndsen, J., 2009. Renaming *Verrucophora farcimen* Eikrem, Edvardsen and Throndsen. *Phycol. Res.* 57, 170.
- Else, P.L., Kraffe, E., 2015. Docosahexaenoic and arachidonic acid peroxidation: it's a within molecule cascade. *Biochim. Biophys. Acta (BBA) - Biomembr.* 1848, 417–421.
- Evensen, Ø., Lorenzen, E., 1997. Simultaneous demonstration of infectious pancreatic necrosis virus (IPNV) and *Flavobacterium psychrophilum* in paraffin-embedded specimens of rainbow trout *Oncorhynchus mykiss* fry by use of paired immunohistochemistry. *Dis. Aquat. Org.* 29, 227–232.
- Fontana, A., d'Impolito, G., Cetignano, A., Miraldo, A., Ianora, A., Romano, G., Cimino, G., 2007. Chemistry of oxylipin pathways in marine diatoms. *Pure Appl. Chem.* 79 (4), 481–490.
- Godratt, A., Rose, A.L., Sarthou, G., Waite, T.D., 2009. New method for the determination of extracellular production of superoxide by marine phytoplankton using the chemiluminescence probes MCLA and red-CLA. *Limnol. Oceanogr. Methods* 7, 682–692.
- González, H.E., Castro, L.R., Dameri, G., Iriarte, J.L., Silva, N., Tapia, F., Teca, E., Vargas, C.A., 2013. Land-ocean gradient in haline stratification and its effect on plankton dynamics and trophic carbon fluxes in Chilean Patagonian fjords (47–50°S). *Prog. Oceanogr.* 119, 32–47.
- Guichardant, M., Chen, P., Liu, M., Calzada, C., Colas, R., Véritel, E., Lagarde, M., 2011. Functional lipids of oxidized products from polyunsaturated fatty acids. *Chem. Phys. Lipids* 164, 544–548.
- Guillard, R.R.L., Hargraves, P.E., 1993. *Stichochrysis immobilis* is a diatom, not a chrysophyte. *Phycologia* 32, 234–236.
- Guindon, S., Dufayard, J.F., Lefort, V., Anisimova, M., Hordijk, W., Gascuel, O., 2010. New algorithms and methods to estimate maximum-likelihood phylogenies: assessing the performance of PhyML 3.0. *Syst. Biol.* 59, 307–321.
- Haigh, N., Esenkulova, S., 2014. Economic losses to the British Columbia salmon aquaculture industry due to harmful algal blooms, 2009–2012. In: Trainer, V.L., Yoshida, T. (Eds.), Proceedings of the Workshop on Economic Impacts of Harmful Algal Blooms on Fisheries and Aquaculture. 47. PICES Sci. Rep. No., pp. 1–6.
- Hallegraeff, G.M., Dorantes-Aranda, J.J., Mardones, J.I., Seger, A., 2017. Review of progress in our understanding of fish-killing microalgae: Implications for management and mitigation. In: Proença, L.A.O., Hallegraeff, G.M. (Eds.), Marine and Fresh-water Harmful Algae. Proceedings of the 17th International Conference on Harmful Algae. International Society for the Study of Harmful Algae and Intergovernmental Oceanographic Commission of UNESCO, Paris, pp. 148–153.
- Herrero, A., Thompson, K.D., Ashby, A., Rodger, H.D., Dagleish, M.P., 2018. Complex gill disease: an emerging syndrome in farmed Atlantic salmon (*Salmo salar* L.). *J. Comp. Pathol.* 163, 23–28.
- Hersbach, H., Bell, B., Berrisford, P., Hirahara, S., Horányi, A., Muñoz-Sabater, J., Nicolas, J., Peubey, C., Radu, R., Schepers, D., Simmons, A., Soci, C., Abdalla, S., Abellán, X., Balsamo, G., Bechtold, P., Biavati, G., Bidlot, J., Bonavita, M., De Chiara, G., Dahlgren, P., Dee, D., Diamantakis, M., Dragani, R., Flemming, J., Forbes, R., Fuentes, M., Geer, A., Haimberger, L., Healy, S., Hogan, R.J., Hölm, E., Janiscová, M., Keeley, S., Laloyaux, P., Lopez, P., Lupu, C., Radnoti, G., de Rosnay, P., Rozum, I., Vamborg, F., Villaume, S., Thépaut, J.-N., 2020. The ERA5 global reanalysis. *Q. J. R. Meteorol. Soc.* 146 (730), 1999–2049.
- Horner, R.A., Garrison, D.L., Plumley, F.G., 1997. Harmful algal blooms and red tide problems on the U.S. west coast. *Limnol. Oceanog.* 42, 1076–1088.
- Hosoi-Tanabe, S., Honda, D., Fukaya, S., Otake, I., Inagaki, Y., Sako, Y., 2007. Proposal of *Pseudochattonella verruculosa* gen. nov., comb. nov. (Dictyochophyceae) for a former raphidophycean alga *Chattonella verruculosa*, based on 18S rDNA phylogeny and ultrastructural characteristics. *Phycol. Res.* 55, 185–192.
- Ikeda, R., Gentleman, R., 1996. A language for data analysis and graphics. *J. Comput. Graph. Stat.* 5, 299–314.
- Imai, I., Yamaguchi, M., Watanabe, M., 1998. Ecophysiology, life cycle and bloom dynamics of *Chattonella* in Seto Inland Sea, Japan. In: Anderson, D.M., Cembella, A., Hallegraeff, G. (Eds.), Physiological Ecology of Harmful Algal Blooms. Springer, Berlin/Heidelberg/New York, pp. 95–112.
- Jakobsen, R., Hansen, P.J., Daugbjerg, N., Andersen, N.G., 2012. The fish-killing dictyochophyte *Pseudochattonella farcimen*: adaptations leading to bloom formation during early spring in Scandinavian waters. *Harmful Algae* 18, 84–95.
- Kim, H.G., 2012. HAB mitigation strategies in Korea and eco-friendly new initiatives. In: Kim, H.G., Reguera, B., Hallegraeff, G.M., Lee, C.K., Han, M.S., Choi, J.K. (Eds.), Harmful Algae 2012: Proceedings of the 15th International Conference on Harmful Algae. International Society for the Study of Harmful Algae, pp. 219–222.
- Larkin, M.A., Blackshields, G., Brown, N.P., Chenna, R., McGettigan, P.A., McWilliams, H., Valentin, F., Wallace, I.M., Wilm, A., Lopez, R., Thompson, J.D., Gibson, T.J., Higgins, D.G., 2007. Clustal W and Clustal X version 2.0. *Bioinformatics* 23, 2947–2948.
- León-Muñoz, J., Urbina, M.A., Garreaud, R., Iriarte, J.L., 2018. Hydroclimatic conditions trigger record harmful algal bloom in western Patagonia (summer 2016). *Sci. Rep.* 8, 1330. <https://doi.org/10.1038/s41598-018-19461-4>.
- Lu, D., Goebel, J., 2000. *Chattonella* sp. bloom in North Sea, Spring 2000. *Harmful Algae News* 21, 10–11.
- Lutz, D.S., 1995. Gas supersaturation and gas bubble trauma in fish downstream from a midwestern reservoir. *Trans. Am. Fish. Soc.* 124 (3), 423–436.
- MacKenzie, L.A., Smith, K.F., Rhodes, L.L., Brown, A., Langi, V., Edgar, M., Lovell, G., Preece, M., 2011. Mortalities of sea-cage salmon (*Oncorhynchus tshawytscha*) due to a bloom of *Pseudochattonella verruculosa* (Dictyochophyceae) in Queen Charlotte sound, New Zealand. *Harmful Algae* 11, 45–53.
- Mansour, M., van Ginkel, S., Dennis, J.C., Mason, B., Elhussin, I., Abbott, K., Pondugula, S.R., Samuel, T., Morrison, E., 2018. The combination of omega-3 stearidonic acid and docetaxel enhances cell death over docetaxel alone in human prostate cancer cells. *J. Cancer* 9 (23), 4536–4546.
- Mardones, J., Clement, A., Rojas, X., 2012. Monitoring potentially ichthyotoxic phytoflagellates in the southern fjords of Chile. *Harmful Algae News* 45, 6–7.
- Mardones, J.I., 2020. Screening of Chilean fish-killing microalgae using a gill cell-based assay. *Lat. Am. J. Res.*, 48(2) <https://doi.org/10.3856/vol48-issue2-fulltext-2400>.
- Mardones, J.I., Dorantes-Aranda, J.J., Nichols, P.D., Hallegraeff, G.M., 2015. Fish gill damage by the dinoflagellate *Alexandrium catenella* from Chilean fjords: synergistic action of ROS and PUFA. *Harmful Algae* 49, 40–49.
- Mardones, J.I., Fuenzalida, G., Zenteno, K., Alves-de-Souza, C., Astuya, A., Dorantes-Aranda, J.J., 2019. Salinity-growth response and ichthyotoxic potency of the Chilean *Pseudochattonella verruculosa*. *Front. Mar. Sci.* 6, 24. <https://doi.org/10.3389/fmars.2019.00024>.
- Mardones, J.I., Norambuena, L., Paredes, J., Fuenzalida, G., Dorantes-Aranda, J.J., Lee Chang, K.J., Guzmán, L., Krock, B., Hallegraeff, G., 2020. Unraveling the *Karenia selliformis* complex with the description of a non-gymnodimine producing Patagonian phylo-type. *Harmful Algae* 98, 101892.
- Marshall, J.-A., Hovenden, M., Oda, T., Hallegraeff, G.M., 2002. Photosynthesis does influence superoxide production in the ichthyotoxic alga *Chattonella marina* (Raphidophyceae). *J. Plankton Res.* 24(11), 1231–1236.
- Marshall, J.-A., Nichols, P.D., Hamilton, B., Lewis, R.J., Hallegraeff, G.M., 2003. Ichthyotoxicity of *Chattonella marina* (Raphidophyceae) to damselfish (*Acanthochromis polyacanthus*): the synergistic role of reactive oxygen species and free fatty acids. *Harmful Algae* 2, 273–281.
- Marshall, J.-A., de Salas, M., Oda, T., Hallegraeff, G., 2005. Superoxide production by marine microalgae. 1. Survey of 37 species from 6 classes. *Mar. Biol.* 147, 533–540.
- Monsen, N.E., Cloern, J.E., Lucas, L.V., Monismith, S.G., 2002. A comment on the use of flushing time, resident time, and age as transport time scales. *Limnol. Oceanogr.* 47 (5), 1545–1553.
- Montes, R.M., Rojas, X., Artacho, P., Tello, A., Quiñones, R.A., 2018. Quantifying harmful algal bloom thresholds for farmed salmon in southern Chile. *Harmful Algae* 77, 55–65.
- Mooney, B.D., Nichols, P.D., de Salas, M.F., Hallegraeff, G.M., 2007. Lipid, fatty acid and sterol composition of eight species of *Kareniaaceae* (Dinophyta): chemotaxonomy and putative phycotoxins. *J. Phycol.* 43, 101–111.
- Naustvoll, L., Dahl, E., Danielssen, D., Aure, J., Skogen, M., Budgell, P., 2002. *Chattonella* i Skagerrak – en ny trussel for oppdrettsnæringen? Havets Miljø. Fisk. og Havet særnummer 2, 126–129.
- Noga, E.J., 2000. Fish Disease: Diagnosis and Treatment. Iowa State University Press, Ames, IA.
- Pagé, B., Pagé, M., Noël, C., 1993. A new fluorometric assay for cytotoxicity measurements in vitro. *Int. J. Oncol.* 3, 473–476.
- Paredes, J., Aguilera, A., Olivares, B., Uribe, C., Urrutia, G., Seguel, M., Villanueva, F., Vargas, M., Varela, D., 2016. Morphological variability and genetic identification of ichthyotoxic species *Pseudochattonella* sp. isolated from severe outbreak in 2016 at the northern Patagonian fjord, southern Chile. Poster presentation at the 17th International Conference on Harmful Algae, Florianópolis, Brazil.
- Pinilla, E., Castillo, M.I., Pérez-Santos, I., Venegas, O., Valle-Levison, A., 2020. Water age variability in a Patagonian fjord. *J. Mar. Sys.* 210, 103376.
- Posada, D., 2008. jModelTest: phylogenetic model averaging. *Mol. Biol. Evol.* 25, 1253–1256.
- Rensel, J.E., Whyte, J.N.C., 2003. Finfish mariculture and harmful algal blooms. In: Anderson, D., Hallegraeff, G., Cembella, A. (Eds.), UNESCO Manual on Harmful Marine Microalgae, 2nd ed. IOC Monographs on Oceanographic Methodology, IOC, pp. 693–722.
- Riisberg, I., Edvardsen, B., 2008. Genetic variation in bloom-forming ichthyotoxic *Pseudochattonella* species (Dictyochophyceae, Heterokonta) using nuclear, mitochondrial and plastid DNA sequence data. *Eur. J. Phycol.* 43 (4), 413–422.
- Ronquist, F., Huelsenbeck, J.P., 2003. MRBayes 3: Bayesian phylogenetic inference under mixed models. *Bioinformatics* 19, 1572–1574.
- Sanz, N., García-Blanco, A., Gavalás-Olea, A., Loures, P., Garrido, J.L., 2015. Phytoplankton pigment biomarkers: HPLC separation using a pentafluorophenyl octadecyl silica column. *Methods Ecol. Evol.* 6, 1199–1209.
- Scholin, C.A., Herzog, M., Anderson, D.M., 1994. Identification of group and strain specific genetic markets for globally distributed *Alexandrium* (Dinophyceae). II. Sequence analysis of a fragment of the LSU rRNA gene. *J. Phycol.* 30, 999–1011.
- Skamarock, W.C., Klemp, J.B., Dudhia, J., Gill, D.O., Barker, D.M., Duda, M.G., Huang, X.-Y., Wang, W., Powers, J.G., 2008. A description of the advanced research WRF version 3. NCAR Technical Note. 475, p. 125.

- Skjelbred, B., Horsberg, T.E., Tollefsen, K.E., Andersen, T., Edvardsen, B., 2011. Toxicity of the ichthyotoxic marine flagellate *Pseudochattonella* (Dictyochophyceae, Heterokonta) assessed by six bioassays. *Harmful Algae* 10, 144–154.
- Smayda, T.J., 1997. What is a bloom? A commentary. *Limnol. Oceanogr.* 42, 1132–1136.
- Smayda, T.J., 2002. Turbulence, watermass stratification and harmful algal blooms: an alternative view and frontal zones as “pelagic seed banks”. *Harmful Algae* 1, 95–112.
- Stien, L.H., Nilsson, J., Hevrøy, E.M., Oppedal, F., Kristiansen, T.S., Lien, A.M., Folkelid, O., 2012. Skirts around a salmon sea cage to reduce infection of salmon lice resulted in low oxygen levels. *Aquac. Eng.* 51, 21–25.
- Strub, P.T., James, C., Montecinos, V., Rutllant, J.A., Blanco, J.L., 2019. Ocean circulation along the southern Chile transition region (38°–46° S): mean, seasonal and interannual variability, with a focus on 2014–2016. *Prog. Ocean.* 172, 159–198.
- Takeoka, H., 1984. Fundamental concepts of exchange and transport time scales in a coastal sea. *Cont. Shelf Res.* 3 (3), 322–326.
- Thomson, P.A., Harrison, P.J., Whyte, J.N.C., 1990. Influence of irradiance on the fatty acid composition of phytoplankton. *J. Phycol.* 26, 278–288.
- Trainer, V., Moore, S.K., Hallegraeff, G., Kudela, R.M., Clément, A., Mardones, J.I., Cochlan, W.P., 2019. Pelagic harmful algal blooms and climate change: lessons from nature's experiments with extremes. *Harmful Algae* 101591. <https://doi.org/10.1016/j.hal.2019.03.009>.
- Vartak, S., McCaw, R., Davis, C.S., Robbins, M.E.C., Spector, A.A., 1998. γ -Linolenic acid (GLA) is cytotoxic to 36B10 malignant rat astrocytoma cells but not to ‘normal’ rat astrocytes. *Br. J. Cancer* 77 (10), 1612–1620.
- Whyte, J.N.C., 1997. Impacts of harmful algae on the west-coast aquaculture industry and a national research plan by the Phycotoxins Working Group of Fisheries and Oceans. *Bull. Aquacult. Assoc. Can.* 97–103.
- Whyte, J.N.C., Haigh, N., Ginther, N.G., Keddy, L.J., 2001. First record of blooms of *Cochlodinium* sp. (Gymnodiniales, Dinophyceae) causing mortality to aquacultured salmon on the west coast of Canada. *Phycologia* 40, 298–304.
- Wichard, T., Poulet, S.A., Halsband-Lenk, C., Albaina, A., Harris, R., Liu, D., Pohnert, G., 2005. Survey of the chemical defense potential of diatoms: screening of fifty one species for α , β , γ , δ -unsaturated aldehydes. *J. Chem. Ecol.* 31, 949–958.
- Xiong, X., Butler, J., Chiang, K., Efremova, B., Fulbright, J., Lei, N., McIntire, J., Oudrari, H., Sun, J., Wang, Z., Wu, A., 2014. VIIRS on-orbit calibration methodology and performance. *Journal of Geophysical Research. Atmospheres* 119 (9), 5065–5078.
- Yamaguchi, M., Itakura, S., Nagasaki, K., Matsuyama, Y., 1997. Effects of temperature and salinity on the growth of the red tide flagellates *Heterocapsa circularisquama* (Dinophyceae) and *Chattonella verruculosa* (Raphidophyceae). *J. Plankton Res.* 19 (8), 1167–1174.
- Yamamoto, C., Tanaka, Y., 1990. Two species of harmful red tide plankton increased in Fukuoka Bay. *Bull. Fukuoka Fish Exp. Stn* 16, 43–44.